UNIVERSITYOF BIRMINGHAM

Mechanical alloying of multi-walled carbon nanotubes reinforced aluminum composite powder

Peng, Tao; Chang, Isaac

[Link to publication on Research at Birmingham portal](#)

Accepted Manuscript

Mechanical Alloying of Multi-walled Carbon Nanotubes Reinforced Aluminum Composite Powder

Tao Peng, Isaac Chang

Mechanical Alloying of Multi-walled Carbon Nanotubes

Reinforced Aluminum Composite Powder

Tao Peng[*], Isaac Chang

School of Metallurgy and Materials, University of Birmingham,

Edgbaston, Birmingham B15 2TT, UK

KEYWORDS: High energy ball milling; Carbon nanotube; CNT; Metal matrix composite; Raman spectrum; Particle size analysis

1. INTRODUCTION

Since the discovery by Sumio Iijima[1] in 1991, carbon nanotube is very attractive to researchers and scientists in view of their extraordinary physical properties and exceptional potential of practical applications. In addition to remarkable chemical and thermal stability, single-walled carbon nanotube (SWNT) has a very high Young's modulus (up to 5 TPa)[2] which is much higher than that of the best known steel (up to 150 GPa)[3]. Although multi-walled carbon nanotube (MWNT) shows lower mechanical properties (Young's modulus is up to 1.8 TPa) than SWNT[4], experimental and theoretical results prove that MWNT is more chemically stable[5] which along with low massive produce prices make MWNT more widely industry applicable.

In order to achieve the full potential of carbon nanotube reinforced metal matrix composite (MMC), several critical issues have to be solved. Homogeneous dispersion of carbon nanotubes in large concentration in metal matrix is the main obstacle due to the strong Van der Waals forces of attraction between long and thin tubes make carbon nanotube vulnerable to agglomerating together. The CNT formed clusters or bundles in matrix deteriorated the overall properties of composite[6]. The other technical problem is the poor interfacial bonding of carbon nanotube and metallic matrix, which is very important for effective load transfer from matrix to CNTs. Especially, weak bonding will lead to the pullout of CNT from Al matrix or fracture at the Al-CNT interface[7].

Numerous research efforts and progresses have been made in the development of carbon nanotubes as reinforcements in ceramic and polymer systems. The interest in using CNT to reinforce metal matrix has been significantly growing over the past few years. Aluminum is remarkable for its low density which is ideal for aerospace and automotive industries however it is severely limited by its low strength. CNT reinforced composites have been projected with metal matrix of aluminum[8-10] by various processing techniques such as mechanical alloying, hot extrusion, hot pressing, equal channel angular pressing (ECAP) and spark plasma sintering to improve the

[*] Corresponding author. Tel: (+44) (0) 121 414 5167. *E-mail address*; ptao.mail@gmail.com (T. Peng).

mechanical performance, especially strength and stiffness while keep light weight[11].

C. F. Deng et al.[12] produced a 1.0 wt. % MWNT-2024Al composite by hot extrusion (733 K, extrusion ratio: 25:1) after isotactic pressing (300 MPa, 10 min). The Young's modulus and tensile strength of the composite increased by 41.3 % and 35.7 % separately comparing with the properties of 2024Al matrix after the same process. M. Jafari and colleagues[13] prepared a 2024Al composite containing 2 vol. % MWNT by high energy ball milling for 4 h and hot pressed at 773 K under a pressure of 250 MPa for 30 min. A maximum compressive strength of 810 MPa was achieved, which is 12 %, 34 % and 78 % higher than that of nanostructured Al2024, Al2024-T6 (artificially aged) and Al2024-O (annealed). More recently, L. L. Cao et al.[14] developed an approach to catalyze pyrolysis of polyethylene glycol and grow CNT on the surface of flake pure Al powders. The as-obtained 2.13 wt. % CNT-Al composite was sintered at 823 K in argon atmosphere for 2 h and then hot pressed at 200 MPa for 30 min. The compressive strength of the as-fabricated composite reached 390 MPa which is two times the strength of the unreinforced Al matrix.

Although a large number of researchers studied CNT-Al composite, most of them put their emphasis on developing different processing techniques and investigating the effects of these techniques on mechanical properties. Very limited studies have been published so far concerning the microstructure of the particles, the evolution of CNT and the processing parameters such as ball milling time and the type of process control agent (PCA) in the processing. Also, some of the techniques can only be operated in a laboratory-scale while some other researchers did not consider the prices of raw materials, which is not economical in large scale industry production. In the present work, the authors chose two different groups of starting materials to compare the microstructure of particles and the dispersion of CNT after the same processing. Mechanical alloying (high energy ball milling) was employed to disperse carbon nanotube in aluminum matrix. 1 wt. % CNT-Al mixture for powder metallurgy use was produced to investigate the evolution of CNT and 1 wt. % CNT-Al composite in the milling process. The effect of process control agents on CNT-Al composite was also studied. The microstructure, such as size, shape and morphology, evolution of the particles were examined by field emission scanning electron microscope (SEM). Raman spectroscope and particle size analyzer were employed to characterize the structure of CNT and statistically calculate the size of particles respectively.

2. EXPERIMENT

2.1 Raw Materials

In order to produce a widely industry capable composite, besides extraordinary properties and performances, the prices of raw materials need to be taken into consideration. Thus, two different groups of starting materials were selected: (A). Aluminum powder (ECKA Granulate GmbH & Co. KG) of purity 99.7 % and powder

size between 75 μm and 106 μm applied by 99 wt. % and multi-walled carbon nanotube (Sigma-Aldrich Co.) of purity > 95 %, diameter 6-9 nm and average length 5 μm applied by 1wt. %; (B) Nano-aluminum powder (The Aluminium Powder Company Ltd, Alpoco) of purity 99.97 % and powder size smaller than 10 μm applied by 99 wt. % and multi-walled carbon nanotube (Cheap Tubes Inc.) with a purity of 90 %, diameter 10-30 nm and average length 10-30 μm applied by 1 wt. %. The composition of each group of the as-proposed Al-1.0 wt. % MWNT composites is shown in Table 1. Group A employed coarse Al powders which are around 50 % cheaper than the fine Al powders in Group B. As a reference, the raw materials in Group B are similar to the materials used by most of other researchers. It is expected that the particles would have similar morphology and microstructure after a certain period of ball milling. A field emission scanning electron microscopy (FESEM) micrograph of the as-received CNTs and a scanning electron microscope (SEM) image of the original aluminum powders are shown in Fig. 1 and Fig. 2 separately.

Table 1 The composition of each group of Al-1.0 wt. % MWNT composites.

2.2 CNT-Al Mixture Preparation

A total weight of 30 g of 99 wt. % aluminum powders and 1 wt. % carbon nanotubes were placed in a 250 ml stainless steel mixing jar under argon atmosphere containing 75 stainless steel ball bearings of 10mm diameter, giving a ball-to-powder weight ratio (BPR) of 10:1. 1 wt. % of stearic acid ($C_{18}H_{36}O_2$) powders or ethanol liquid were put into the milling pot as process control agent to prevent the excessive cold welding of Al powders. Then the ball milling pot was fixed and agitated on a planetary ball mill (Glen Creston Ltd, FRITSCH, Pulwerisette 5) running at a constant speed of 250 rpm with an interim period of 10 min for every 20 min's milling in order to prohibit over-heating. After a certain period of milling, all the mixtures were taken out from the milling pot instead of taking a small amount of mixtures as samples and continuing ball milling.

2.3 Characterization Methods

The shape and morphology of as-milled powders were characterized by Philips XL-30 scanning electron microscopy (SEM) and JEOL 7000 field emission scanning electron microscopy (FESEM). The size distribution of as-milled powders was determined by particle size analyzer (Sympatec, Sensor: QICPIC). The structure of carbon nanotube was analyzed by RENISHAW inVia Raman spectroscope with a 532 nm line of Nd: YAG laser as excitation source.

3.   RESULTS AND DISCUSSION

3.1 Raw Materials

Fig. 1 SEM images showing clusters of raw carbon nanotubes. (a) for CNT in Group A materials; (b) for CNT in Group B materials.

Fig. 1 shows the SEM micrographs of raw carbon nanotubes, it is clear that the tangled and curved CNT were agglomerated together as big clusters due to the strong Van der Waal force between the long and thin tubes. The agglomeration of CNT is one of the biggest challenges for CNT reinforced composites which leads to premature crack initiation and fracture in tension. In the authors' endeavor, CNT bundles are expected to be separated and uniformly dispersed in aluminum metal matrix by high energy ball milling [8, 15].

Fig. 2 SEM images of morphology and shape of the original aluminum powder: (a) and (b) for aluminum powder of Group A; (c) and (d) for aluminum powder of Group B.

The morphology and shape of the starting aluminum powder is showed in Fig. 2. As can be seen from the images, the aluminum powders in Group A have irregular shape and very rough surfaces while the aluminum powders of Group B have much smaller particle size and uniformly clean and smooth surfaces. The author expected the rough Al powders from Group A with a lot of bulges and hollows can trap a certain amount of carbon nanotubes and then wrap CNT inside Al particles protecting CNT from being damaged, thus achieving better properties of the Al- 1 wt.% MWNT composite. In contrast, the CNT in smooth Al powders from Group B may be seriously broken by the high energy milling balls due to a lack of attachment. The smooth surfaces allow CNTs to stand on their own and separate from Al particles, which exposes CNTs to the fierce collision of high speed moving ball bearings. This will increase the defects and dislocations in the as-added CNT and, consequently, transfer lower properties of CNT into the Al matrix.

3.2 The Effect of Process Control Agent

Fig. 3 SEM images of aluminum powder milled for 5 h without the addition of PCA. (a) for Group A and (b) for Group B.

To investigate the effect of process control agents on the as-milled particles, pure aluminum powders with 1 wt. % CNT were milled without any process control agent for 5 h (Fig. 3). As can be seen in Fig. 3(a) that the surfaces of the particles in Group A became smoother than the raw Al powder, the particle shape became spherical and the size approached 2 mm. In Fig. 3(b), the as-milled Al particles of Group B, similar to Group A, also increased in size but with a wider distribution range. Some of these particles even reached 1 mm though their shapes are irregular. The changes in particles

4

size can be seen more clearly from the cumulative particle size distribution (Table 2). D_{50}, the average median diameter, was chose to compare the representative particle sizes of ball-milling or MA products, which is also used by other researchers[15]. Evidently from Table 2 that the D_{50} of particles increased significantly from the starting 91.87 μm and 9.92 μm to 2 mm and around 1 mm for powders, after being ball milled for 5 h, in Group A and Group B separately.

Table 2 The D_{50} of different particles (μm).

However, the Al powders milled with 1 wt. % CNT and 1 wt. % process control agent for the same 5 h showed totally different outcome. Despite the shape and morphology of particles which is discussed in the following section, according to Table 2, the addition of 1 wt. % stearic acid reduced the D_{50} of as-milled powders to 112 μm and 38 μm for Group A and Group B individually. The addition of 1 wt. % ethanol as PCA achieved even greater refinement effect after being high energy ball milled for 5 h that the D_{50} of as-milled Al powders reached 13.74 μm and 8.02 μm for Group A and Group B respectively.

The reason for the growth of particle size is the excessive cold welding of ductile Al powder in the mechanical alloying process. High speed running ball bearings not only deformed the soft Al particles but also welded them together when the clean and flat surfaces were brought into contact, which lead to the increase of particle size after milling. In contrast, the addition of PCA (e.g. ethanol or stearic acid) dispersed evenly in the metal matrix and gradually covered the Al particles' surfaces during ball milling process, which formed a barrier for cold welding process by preventing the contact of fresh surfaces of Al particles. Also, the PCA reduced the tendency of welding between ductile Al powders and stainless steel ball bearings/inner walls of milling pots[16]. Hence the presence of PCA leads to a smaller particle size as compared to those powders milled without PCA.

3.3 The Effect of Ethanol and Stearic Acid

Fig. 4 Cumulative particle size distribution of pure Al powders and Al-1 wt.% CNT mixture with 1 wt. % ethanol as process control agent for different milling time. (a) for Group A materials and (b) for Group B materials.

Fig. 4 and Fig. 5 show plots of cumulative particle size distribution of pure Al powders and Al-1 wt. % CNT with 1 wt. % ethanol and 1 wt. % stearic acid as process control agent for different ball milling time, respectively. It is worth noticing that the particle size is different, despite in Group A or Group B, after milling for the same time when different process control agents were applied. As can be seen from Table 2, Fig. 4(a) and Fig. 5(a) that, with the addition of 1 wt. % stearic acid, particle size of Group A

powders reached 112.83 μm and 59.78 μm after being ball milled for 5 h and 10 h respectively. Meanwhile, for the same Al-1 wt.% CNT powders milled with 1 wt. % ethanol, the particle size also decreased, but more significantly, to 13.74 μm and 2.43 μm after milling for the same 5 h and 10 h individually. Similar trend can be found in Fig. 4(b) and Fig. 5(b) that the particles of Group B became much finer (8.02 μm and 2.64 μm for the milling time of 5 h and 10 h separately) when milled with 1 wt. % ethanol, whereas the particles size is larger (38.03 μm and 55.95 μm for the milling time of 5 h and 10 h separately) with the aid of 1 wt. % stearic acid and milled for the same milling time length. These results indicate that 1 wt. % ethanol is more effective in refining particles in high energy ball milling than 1 wt. % stearic acid.

Fig. 5 Cumulative particle size distribution of pure Al powders and CNT-Al mixture with 1 wt. % stearic acid as process control agent for different milling time. (a) for Group A materials and (b) for Group B materials.

The reason for the different impact of stearic acid and ethanol on ball-milled particles is not fully understood yet. But possible mechanisms may be proposed and tested in the future. It is reported[17] that PCA is most effective in the early stage of MA process and a liquid state PCA can reach the required sites faster comparing to the solid phase PCA. Ethanol has a melting point of 159 K and exists in the milling pot as liquid while the melting point of stearic acid is 340 K–342 K which is in the solid state in the pot. Fluid molecules of ethanol would wet the surfaces of CNT-Al mixtures and even flow into cracks on the particles once they are put into the milling pot. On the contrary, stearic acid as solid particles needs to be broken apart first and gradually mix with the Al-1 wt. % CNT powders, which slow down the welding prevention process. Another possible explanation is the different molecule size which affects the absorption of PCA on mixture surfaces[18]. A ethanol molecule (C_2H_5OH) has 5 C-H bonds whereas a stearic acid molecule ($CH_3(CH_2)_{16}COOH$) has 35 C-H bonds. Based on the length and angle of C-H bond, it can be easily understood that the stearic acid molecule is much bigger than ethanol molecule. Therefore, individual ethanol molecule is more free-moved than strearic acid in the metallic matrix. Also, there were a larger amount of ethanol molecules than stearic acid molecules for the same 1 wt. % weight, which makes ethanol more effective in preventing excessive cold welding of ductile Al particles. To sum up, good mobility makes ethanol more efficient in decreasing particle size than stearic acid.

3.4 The Evolution of Aluminum Powder

Fig. 6 SEM images showing particle morphology of CNT-Al mixture for various milling time with the addition of 1 wt. % stearic acid : (a) – (d) for Group A materials, (e) – (h) for Group B materials.

In general mechanical alloying, there are two competing processes: fracturing and cold welding. Fracturing would decrease ductility and finally lead to small particle size

while cold welding would produce large particle size. It is common for the MA processing to be dominated by cold welding process resulting agglomeration of particles where PCAs were employed to balance cold welding and fracturing as well as improve the process efficiency.

The morphology and size evolution of Al powder after being high energy ball-milled for different milling time with the addition of 1 wt. % stearic acid and 1 wt. % CNT is showed in Fig. 6(a) to Fig. 6(d). It can be seen by comparing Fig. 2(a) and Fig. 6(a) that large raw Al powders in Group A were first flattened into flake shape reached at a size of 153.70 μm after being milled for 1 h. Although the laminar morphology remained [Fig. 6(b)], the size of particles milled for 5 h decreased to 112.83 μm and the surfaces became rougher comparing to the particles milled for 1 h. Also, the particle size distribution of 5 h-milled powders became wider than that of 1 h-milled powders which can be seen obviously from Fig. 5(a), which is due to the fracturing of big particles and the cold welding of small particles. With the milling time increased to 10 h, the shape of particles became irregular and ununiformed in Fig. 6(c) while the size kept down to 59.78 μm. At this stage, big flaky powders were almost broken by the collision of ball bearings and particles. The small fragments welded one on the other to build relatively equiaxed particles. After 20 h of ball milling, the particle size became more even [Fig. 6(b)] and the distribution of particles became narrower which is apparently in Fig. 5(a). This suggests cold welding and fracturing reached a state of equilibrium.

In contrast to the case of materials from Group A, different behaviors of particles were observed in powders from Group B as shown in Fig. 6(e) to Fig. 6(h), in which the size of particles kept an increasing trend. It can be observed that the powders with a spherical morphology in Fig. 2(b), typical gas-atomized powders, were first flattened in the early stage while particles size increased from 9.92 μm for raw Al powders to 10.58 μm after milling for 1 h, which is similar to the initial stage of ball milled Group B materials. However, with the increase of milling time to 5 h and 10 h, the particle size of Group B powders further grew to 38.03 μm and 55.95 μm respectively, which is opposite to the tendency of as-milled Group A powders. This along with the narrowing of particle size distribution in Fig. 5(b) suggest that powders increased in size by coalescing the smaller powders[15]. After 20 h of milling, particles that welded by several flaky particles can be apparently seen in Fig. 6(h). Despite the size of starting materials is different, the size of particles from Group A and Group B, both with 1 wt. % stearic acid, reached around 65 μm after high energy ball milling for 20 h. The authors expect the 20 h-milled powders from both groups will have similar mechanical properties, which will be investigated in the following experiments. The reason for keeping the increasing trend of particle size may be due to the limitations of the milling ball bearings. It is stated by other scholars[17] that a certain diameter of grinding ball can only produce a certain size of particles. Reduce the diameter of the ball bearing may further refine the particles.

Fig. 7 SEM images showing particle morphology of CNT-Al mixture for various milling time with the addition of 1 wt. % ethanol : (a) – (c) for Group A material, (d) – (f) for Group B material.

Regarding the milling groups that employed 1 wt. % ethanol as PCA, the particle size from Group A mixture was first increased then significantly decreased while the particle size from Group B powders was decreased all the way with the increase of milling time as can be seen in Fig. 7. It is obvious that the particles in Group A that ball milled for 1 h have a disc-like shape and smooth edges which is showed in Fig. 7(a). Similar to the milling with 1 wt. % stearic acid as PCA, the particle size of Group A with 1 wt. % ethanol was initially grew to 146.50 μm after milling for 1 h and then decreased to 13.74 μm and 2.43 μm for 5 h and 10 h of milling respectively. Nevertheless, the particle size of Group B milled with 1 wt. % ethanol kept decrease from 9.92 μm for the raw Al powder size to 9.72 μm after milling for 1 h. With the milling time increasing to 5 h and 10 h, the particle size dropped to 8.02 μm and 2.64 μm individually. The fine as-milled powders in Fig. 7(c) and Fig. 7(f) are ideal for the following consolidation process such as sintering and equal-channel angular pressing (ECAP) which is the subject of ongoing study by the author, however, the particle refinement will have some negative effects to the structure of CNT which   is discussed in detail in the following paragraphs.

3.5 The Evolution of Carbon Nanotube

The dispersion of CNT in Al matrix is characterized by FESEM as showed in Fig. 8. As can be seen from Fig. 8(a) and Fig. 8(b), for both Group A and Group B materials with 1 wt. % stearic acid as PCA after milling for 1 h, big MWNT agglomerates randomly exist on the surface of Al particles and between Al particles. The size of the clusters decreased moderately but obvious agglomeration is still visible after milling for 5 h as shown in Fig. 8(b). When the milling continued to 10 h, the CNT bundles disappeared and individual CNT can be found embedded on the surface of the Al particle [Fig. 8(d)]. This indicates the homogenous distribution of CNT in Al mixture which also suggests that mechanical alloying or ball milling is effective in disperse CNT in Al powder. The carbon nanotube cannot be seen from FESEM micrographs after ball milling for 20 h. The authors deem that CNTs were covered by ductile Al matrix after long time milling as other researchers[19] who fractured 48 h ball-milled CNT-Al particles and find individual CNT in the Al matrix. The existence of CNT after ball milling for 20 h was proved by the Raman spectrum.

Fig. 8 SEM images showing the distribution of CNT in as-milled CNT-Al matrix.(a), (b) and (d) for Group B materials with 1 wt.% stearic acid milled for 1h, 5h and 10h. (c) for Group A materials with 1 wt.% stearic acid milled for 1h.

Fig. 9 Raman spectra of pure Al powders and CNT-Al mixture powders with the addition of 1 wt. %

8

stearic acid for different milling time. (a) for Group A materials, (b) for Group B materials.

Fig. 10 Raman spectra of pure Al powders and CNT-Al mixture powders with the addition of 1 wt. % ethanol for different milling time. (a) for Group A materials, (b) for Group B materials.

Raman spectroscope is used to reveal the complementary information on the evolution of CNT after each milling. In Raman spectrum of CNT, the first order peaks exhibit the structure information of CNT which composed of D band at around 1350 cm^{-1} and G band that is typically located at 1580 cm^{-1}[20]. G band is observed for perfect hexagonal graphite and will therefore appear wider and smaller for badly structured and defect containing nanotubes. On the other hand, D band is attributed to lattice defects and finite crystal size which related to a breaking of the 2D translational symmetry, so that it will increase and broadened with increasing number of defects in the nanotubes[20]. The broadening of the D and G peaks observed here also indicates amorphisation of the nanotubes in the ball milling process. Fig. 9 and Fig. 10 present the Raman spectrum of CNT with different PCA and milled for different time.

Table 3 The I_D/I_G ratio of raw CNT and Al-1 wt. % CNT mixture powders with the addition of 1 wt. % stearic acid for different milling time.

Table 4 The I_D/I_G ratio of raw CNT and Al-1 wt. % CNT mixture powders with the addition of 1 wt. % ethanol for different milling time.

The intensity ratio of D band peak and G band peak (I_D/I_G) is often used to assess and evaluate the structure of CNT. The more hexagonal graphite (the higher the G band peaks) and less defects (the lower the D band peaks) exist, the lower I_D/I_G will be and the better mechanical properties will be achieved in the final product. Table 3 and Table 4 depict the I_D/I_G of different groups under certain milling conditions. It is worth noticing that the D band and G band peaks can be detected on any particles that the author chose to test, which also proved the homogenous distribution of CNT in Al metal matrix after milling for a certain time.

It can be seen that the I_D/I_G ratio rose after a period of milling. As showed in Table 3, the I_D/I_G of Group A with 1 wt. % stearic acid as PCA increased from 0.85 for raw MWNT to around 0.98 after milling for 5 h and 10 h before reaching 1.08 at 20 h. The starting I_D/I_G of Group B materials is higher than that of Group A, but as the milling continued, this ratio is approaching at 0.98 for milling for 5 h. The I_D/I_G of groups with the addition of 1 wt. % ethanol in Table 4 also display similar gradually growing trend. The climb of I_D/I_G indicates the damage of the graphite structure, which will deteriorate the strength and stiffness of the CNT reinforced composite. Perfect CNT structure can better translate the excellent performance of CNT into composite materials. So effort should

9

be made to protect CNT from being broken during the ball milling process.

Comparing the same material groups with 1 wt. % different PCAs milling for the same time, it is clear that the I_D/I_G of groups adding 1 wt. % ethanol is higher than that of groups milled with 1 wt. % stearic acid. The I_D/I_G of Group A with 1 wt. % ethanol increased to 1.11 after milling for 5 h and peaked at 1.12 for 10 h whereas the ratio of this group with 1 wt. % stearic acid grew a little to 0.98 and 0.97 after milling for 5 h and 10 h separately. Similarly, the I_D/I_G of Group B with 1 wt. % ethanol reached at 1.03 after milling for 10 h, while this ratio was only 0.98 for the same Group adding 1 wt. % stearic acid for the same milling time. This exceed of ratio for 1 wt. % ethanol added material groups means that the 1 wt. % CNT milled with 1 wt. % ethanol in the Al powder was more severely damaged than milled with 1 wt. % stearic acid. Although fine powders can be achieved in the groups with 1 wt. % ethanol as process control agent, the structure of CNT were more seriously broken than the groups with 1 wt. % stearic acid. The balance between particle size and the structure of CNT needs to be solved which will be investigate in the author's future study.

4. CONCLUSIONS

The results presented in this paper demonstrate that mechanical alloying is an effective way of dispersing CNTs in aluminum matrix. Homogeneously dispersed Al-1 wt. % CNT mixtures were achieved by high energy ball milling. It was found from Raman spectra that ball milling induced defects into CNT structure. The use of process control agents such as 1 wt. % ethanol and 1 wt. % stearic acid helped keep particles separated and decrease agglomeration of Al powders. Especially, adding 1 wt. % ethanol can achieve more fine particles whereas adding 1 wt. % stearic acid can better preserve the tubular structure of CNT than 1 wt. % ethanol.

5. ACKNOWLEDGMENT

REFERENCE

[1] S. Iijima, Helical Microtubules of Graphitic Carbon, Nature, 354 (1991) 56-58.

[2] V.N. Popov, Carbon nanotubes: properties and application, Materials Science & Engineering R-Reports, 43 (2004) 61-102.

[3] D. Poirier, R. Gauvin, R.A.L. Drew, Structural characterization of a mechanically milled carbon nanotube/aluminum mixture, Composites Part a-Applied Science and Manufacturing, 40 (2009) 1482-1489.

[4] R. George, K.T. Kashyap, R. Raw, S. Yamdagni, Strengthening in carbon nanotube/aluminium (CNT/Al) composites, Scripta Materialia, 53 (2005) 1159-1163.

[5] A.H. Javadi, S. Mirdamadi, M.A. Faghihisani, S. Shakhesi, R. Soltani, Fabrication of well-dispersed, multiwall carbon nanotube-reinforced aluminum matrix composites, New Carbon Materials, 27 (2012) 161-165.

[6] J.Z. Liao, M.J. Tan, Mixing of carbon nanotubes (CNTs) and aluminum powder for powder metallurgy use, Powder Technology, 208 (2011) 42-48.

[7] A.M.K. Esawi, M.M. Farag, Carbon nanotube reinforced composites: Potential and current challenges, Materials & Design, 28 (2007) 2394-2401.

[8] A. Esawi, K. Morsi, Dispersion of carbon nanotubes (CNTs) in aluminum powder, Composites Part a-Applied Science and Manufacturing, 38 (2007) 646-650.

[9] K. Morsi, A. Esawi, Effect of mechanical alloying time and carbon nanotube (CNT) content on the evolution of aluminum (Al)-CNT composite powders, Journal of Materials Science, 42 (2007) 4954-4959.

[10] A.M.K. Esawi, K. Morsi, A. Sayed, A.A. Gawad, P. Borah, Fabrication and properties of dispersed carbon nanotube-aluminum composites, Materials Science and Engineering a-Structural Materials Properties Microstructure and Processing, 508 (2009) 167-173.

[11] S.R. Bakshi, V. Singh, S. Seal, A. Agarwal, Aluminum composite reinforced with multiwalled carbon nanotubes from plasma spraying of spray dried powders, Surface and Coatings Technology, 203 (2009) 1544-1554.

[12] C.F. Deng, D.Z. Wang, X.X. Zhang, A.B. Li, Processing and properties of carbon nanotubes reinforced aluminum composites, Materials Science and Engineering a-Structural Materials Properties Microstructure and Processing, 444 (2007) 138-145.

[13] M. Jafari, M.H. Abbasi, M.H. Enayati, F. Karimzadeh, Mechanical properties of nanostructured Al2024-MWCNT composite prepared by optimized mechanical milling and hot pressing methods, Advanced Powder Technology, 23 (2012) 205-210.

[14] L.L. Cao, Z.Q. Li, G.L. Fan, L. Jiang, D. Zhang, W.J. Moon, Y.S. Kim, The growth of carbon nanotubes in aluminum powders by the catalytic pyrolysis of polyethylene glycol, Carbon, 50 (2012) 1057-1062.

[15] L. Wang, H. Choi, J. M. Myoung, W. Lee, Mechanical alloying of multi-walled carbon nanotubes and aluminium powders for the preparation of carbon/metal composites, Carbon, 47 (2009) 3427-3433.

[16] P.S. Gilman, W.D. Nix, The structure and properties of aluminum alloys produced by mechanical alloying: Powder processing and resultant powder structures, Metallurgical Transactions A, 12 (1981) 813-824.

[17] P.R. Soni, Mechanical Alloying: Fundamentals and Applications, 2000.

[18] W. Lee, S.I. Kwun, The effects of process control agents on mechanical alloying mechanisms in the Ti ・ Al system, Journal of Alloys and Compounds, 240 (1996) 193-199.

[19] D. Zheng, J.S. Ye, W.D. Zhang, Some properties of sodium dodecyl sulfate functionalized multiwalled carbon nanotubes electrode and its application on detection of dopamine in the presence of ascorbic acid, Electroanal, 20 (2008) 1811-1818.

[20] D.L.a.A.A. S. R. Bakshi, Carbon nanotube reinforced metal matrix composites – a review, International Materials Reviews, 55 (2010) 41-64.

Table 1 The composition of each group

	99 wt. % Aluminium Powder		1 wt. % Carbon Nanotube		
	Particle Size (µm)	Purity (%)	Diameter (nm)	Length (µm)	Purity (%)
Group A	75-106	99.7	6-9	5	>95
Group B	Up to 10	99.97	10-30	10-30	90

Table 2 The D_{50} of different particles (μm)

Process Control Agent	Non	Stearic Acid				Ethanol		
Milling Time (h)	0	1	5	10	20	1	5	10
D_{50} of Group A (μm)	91.87	153.70	112.83	59.78	62.10	146.50	13.74	2.43
D_{50} of Group B (μm)	9.92	10.58	38.03	55.95	75.73	9.72	8.02	2.64

Table 3 The I_D/I_G ratio of raw CNT and Al-1 wt. % CNT mixture powders with the addition of 1 wt. % stearic acid for different milling time.

Milling Time	0 h	1h	5h	10h	20h
Group A	0.85	0.87	0.98	0.97	1.08
Group B	0.90	0.95	0.98	0.98	1.03

14

Table 4 The I_D/I_G ratio of raw Al powders and CNT-Al mixture powders with the addition of 1 wt. % ethanol for different milling time.

Milling Time	0 h	1h	5h	10h
Group A	0.85	0.94	1.12	1.11
Group B	0.90	1.01	1.01	1.03

Fig. 1
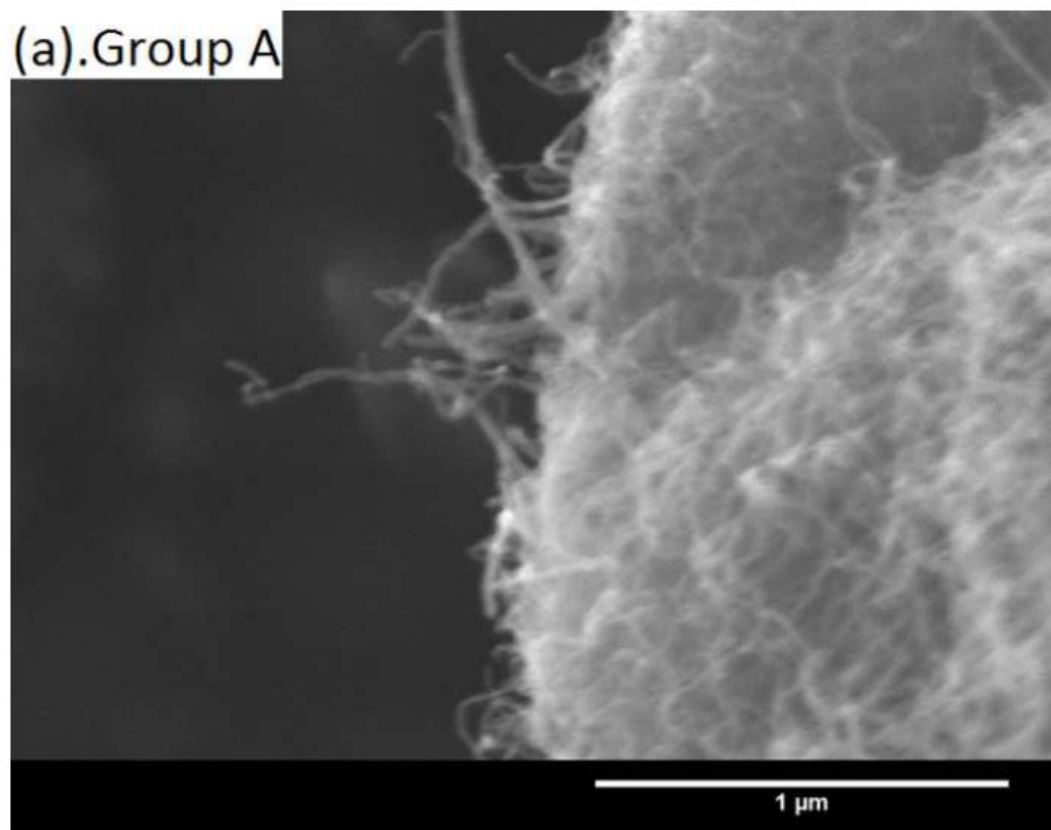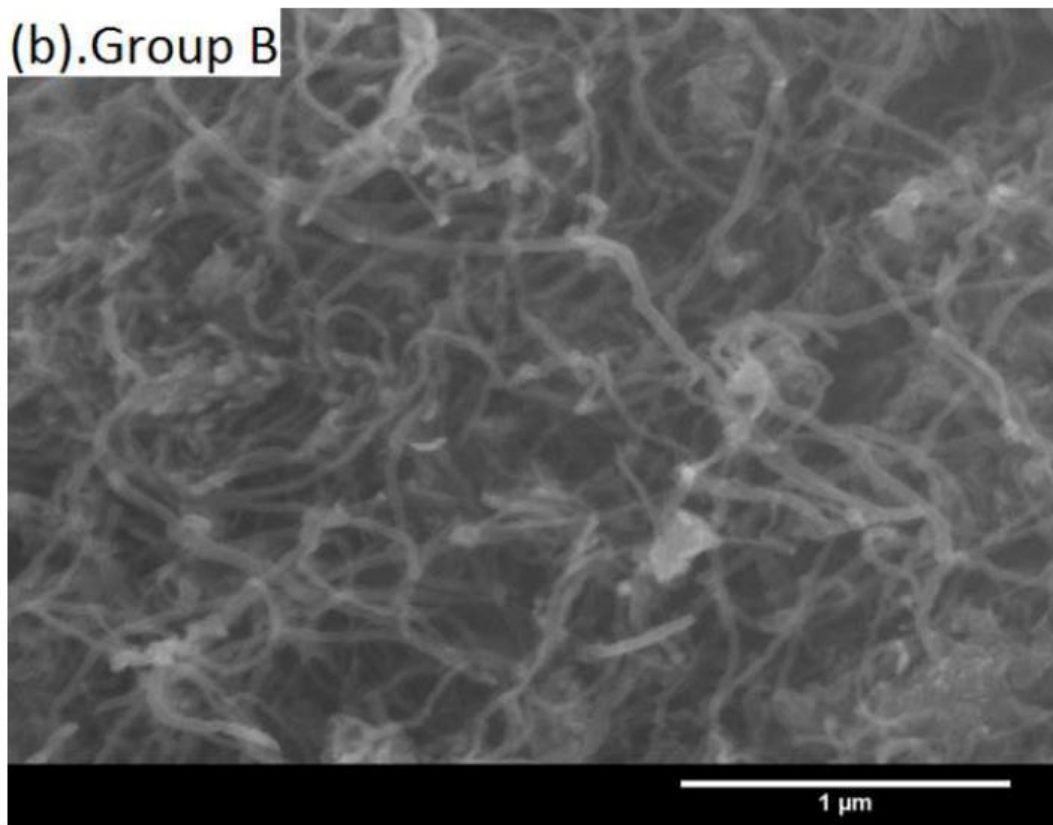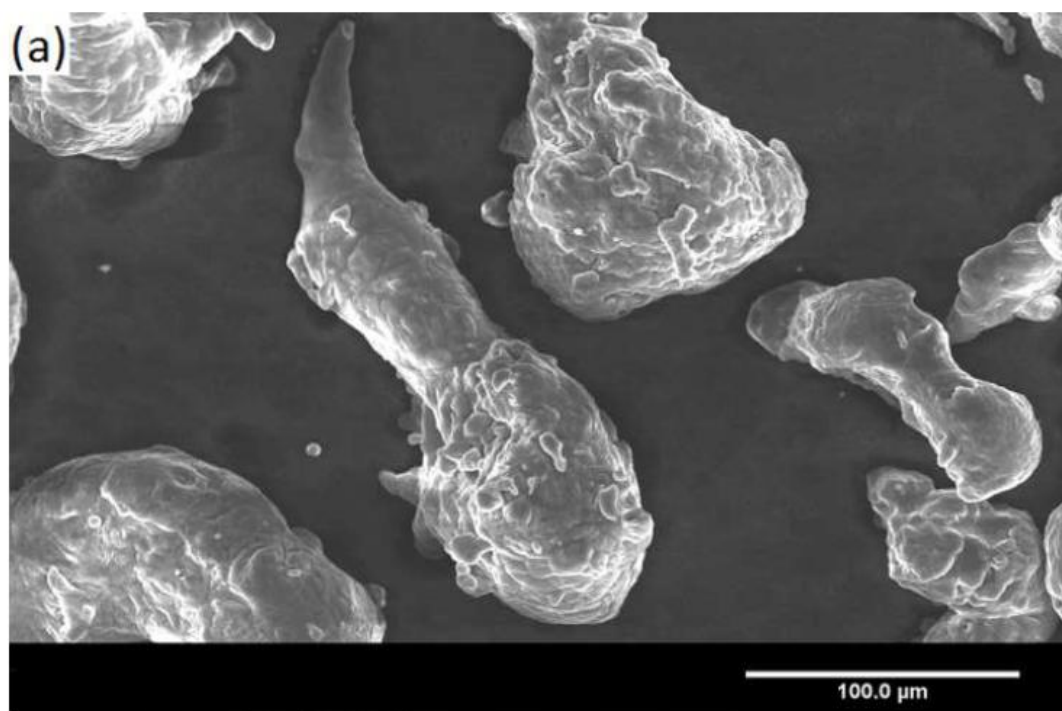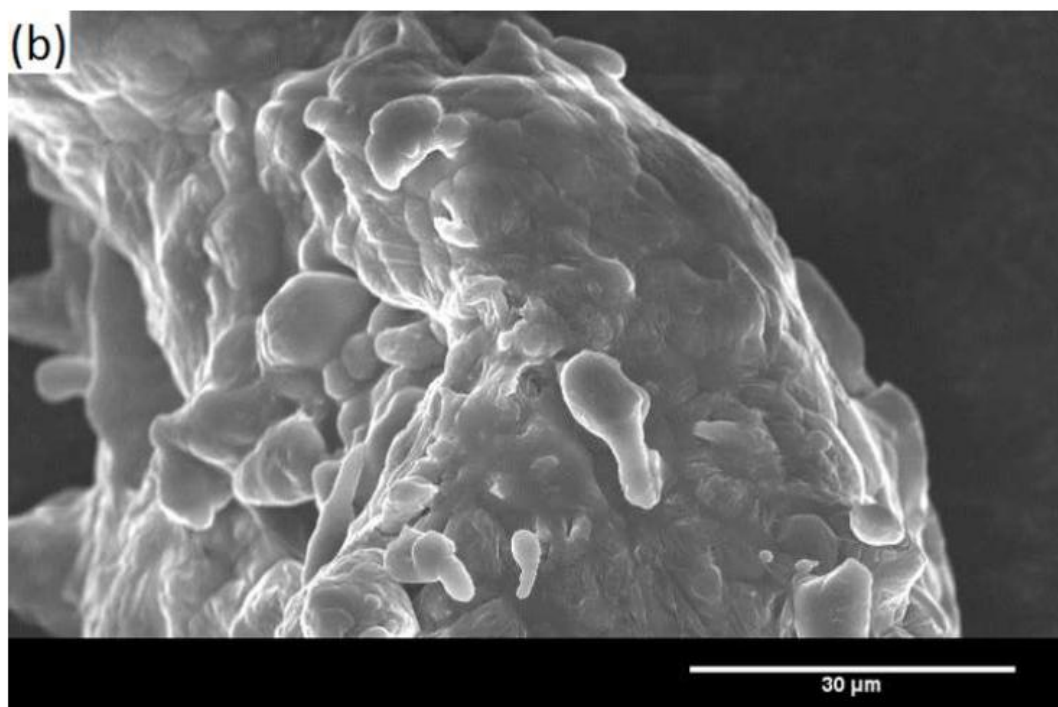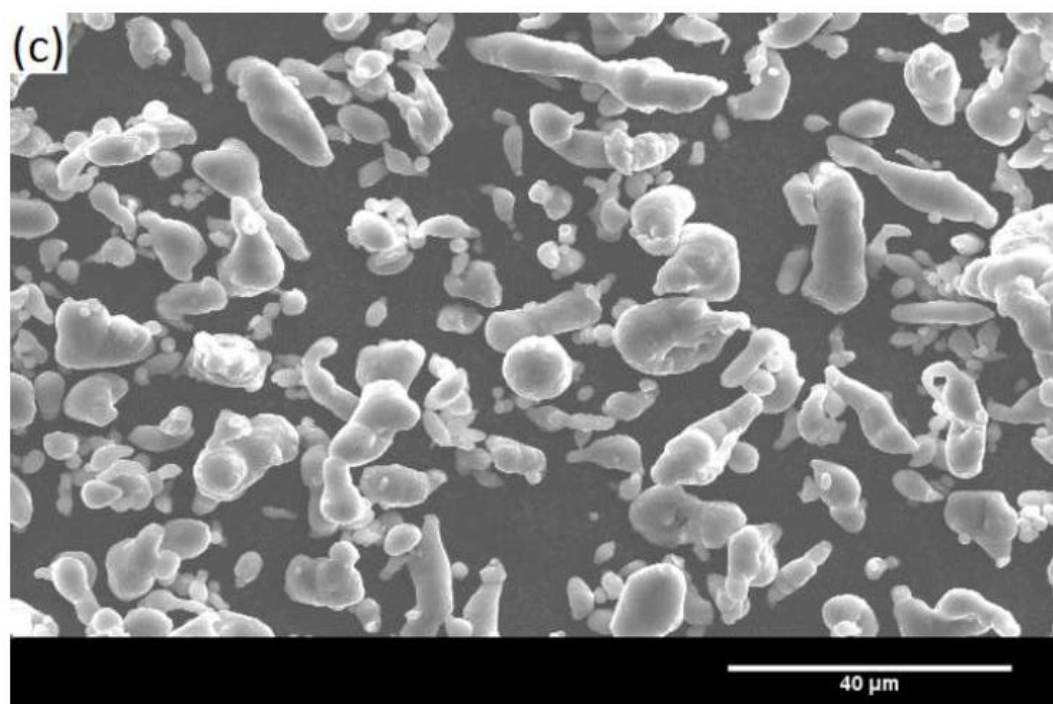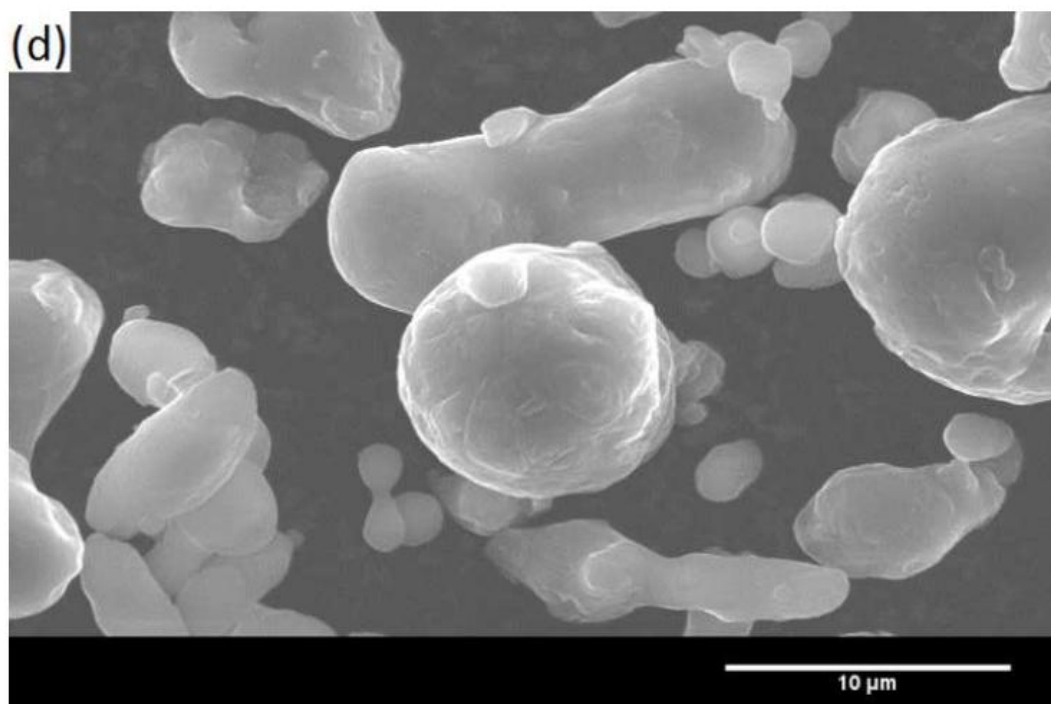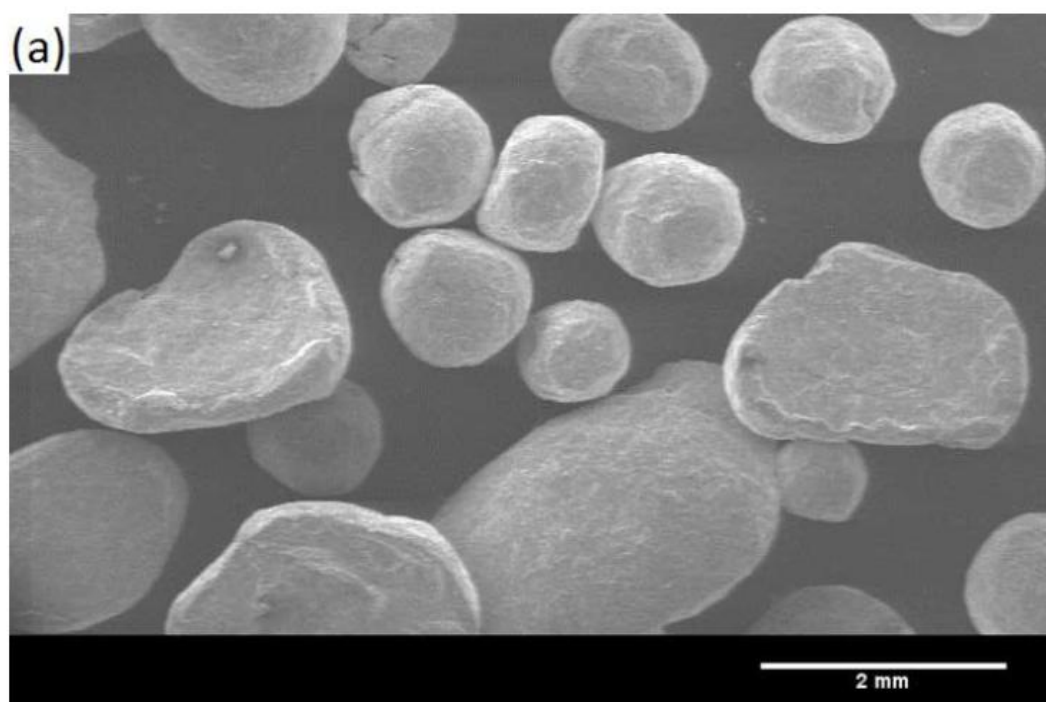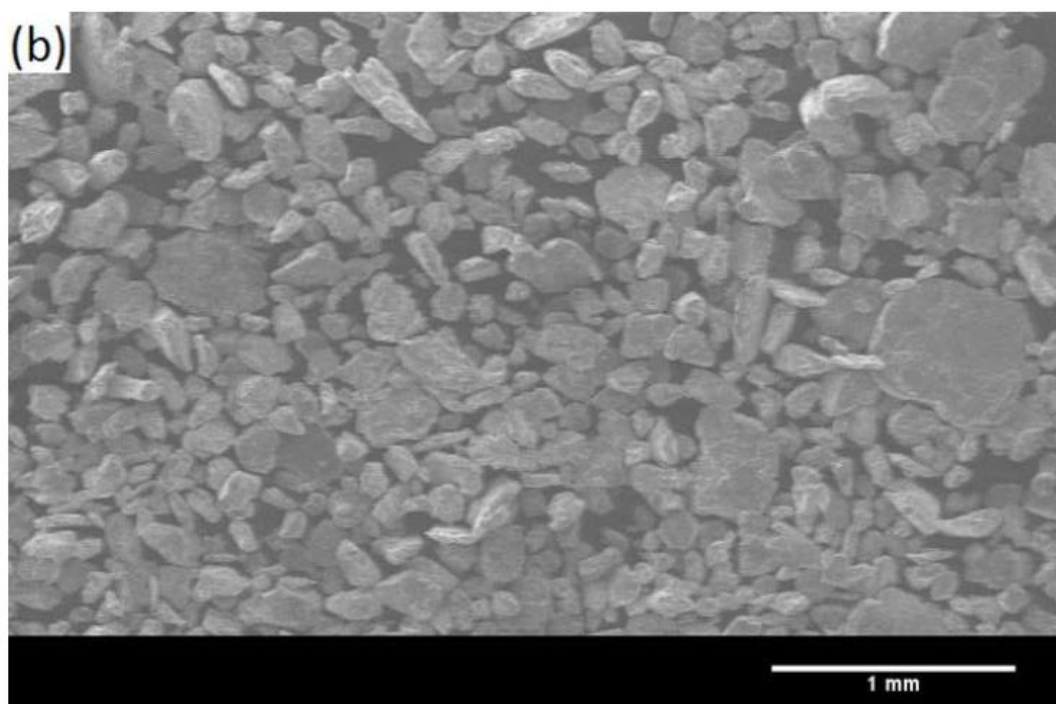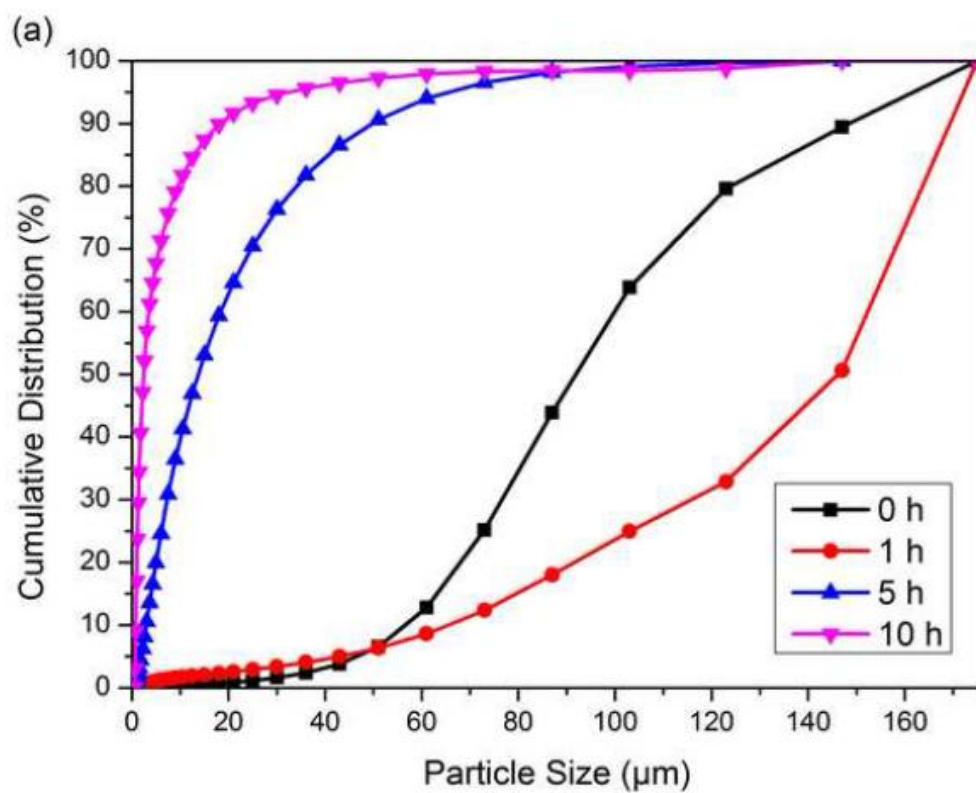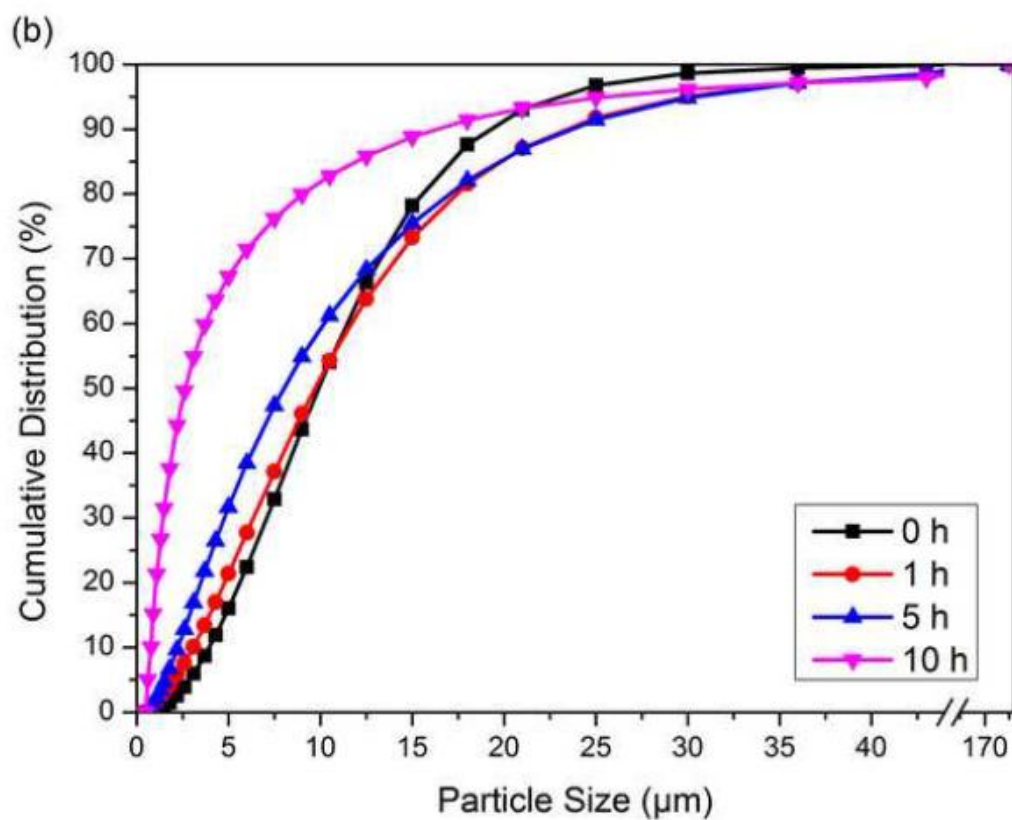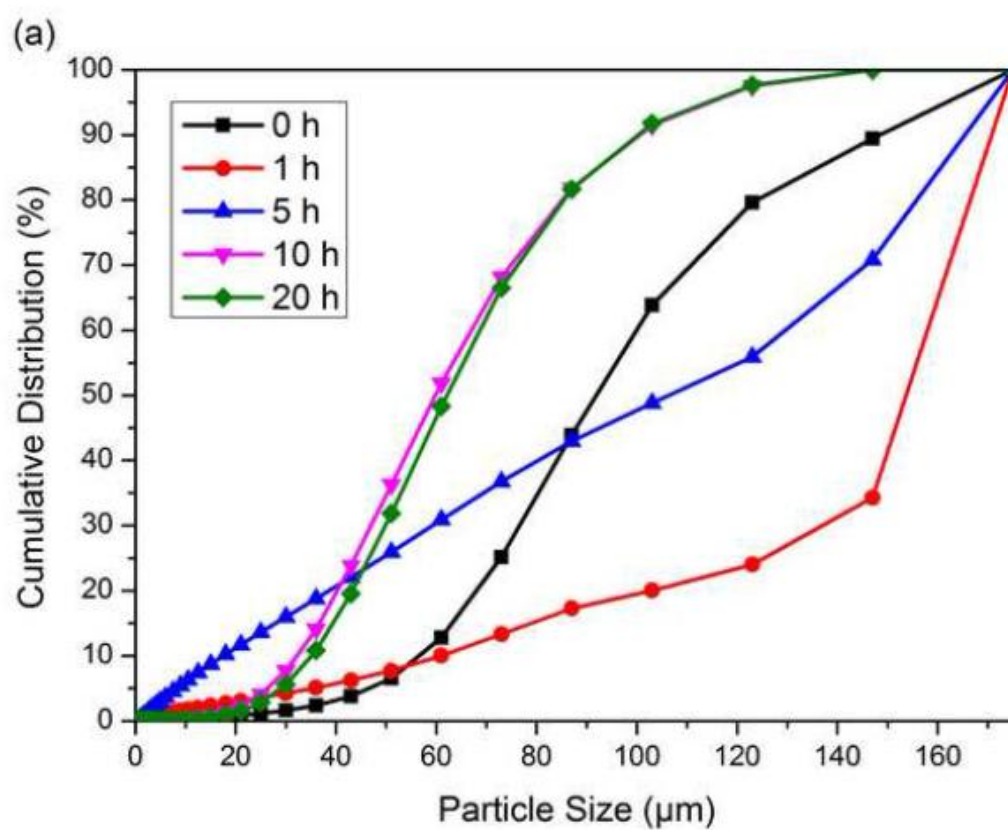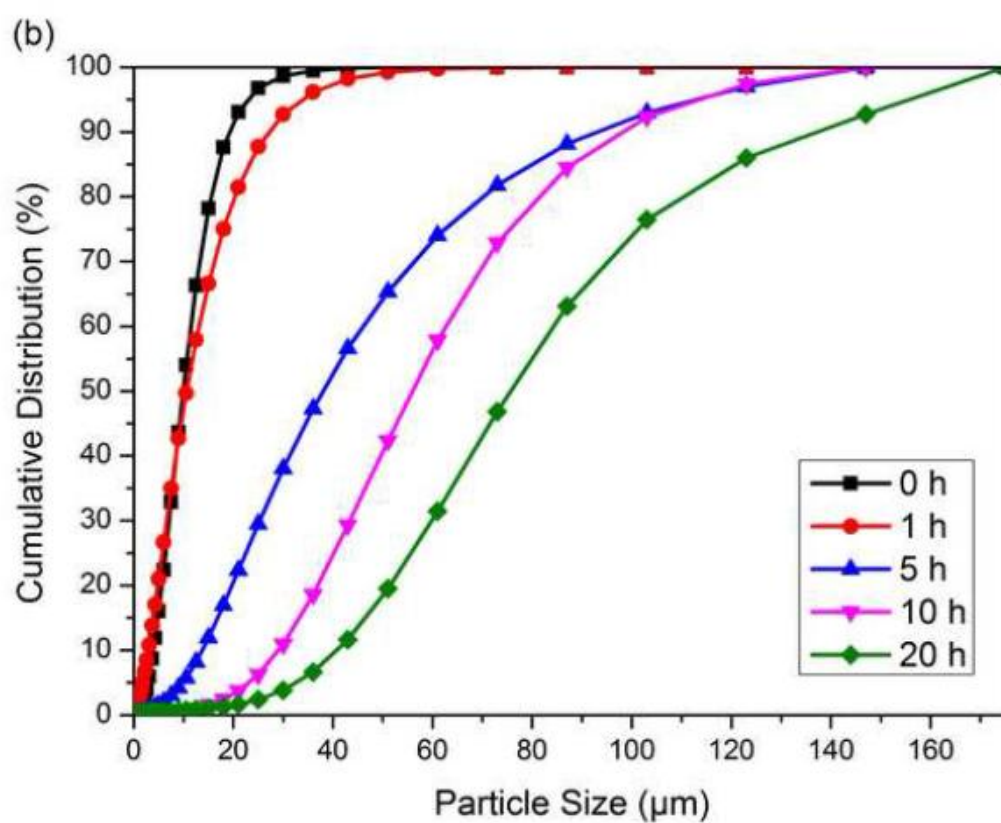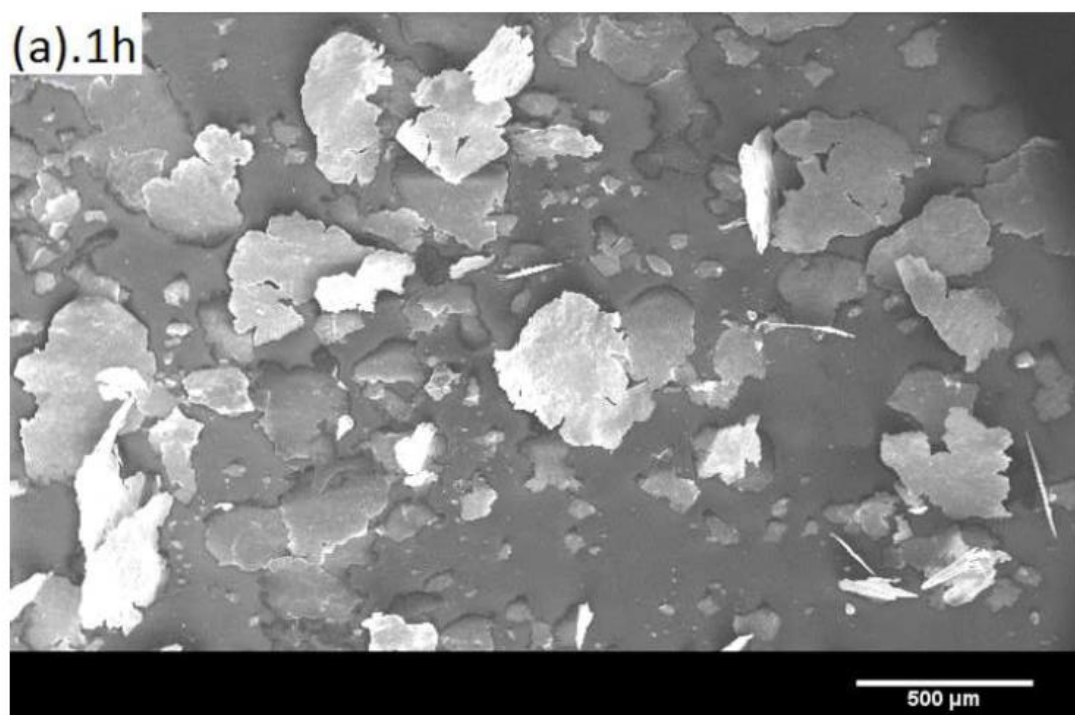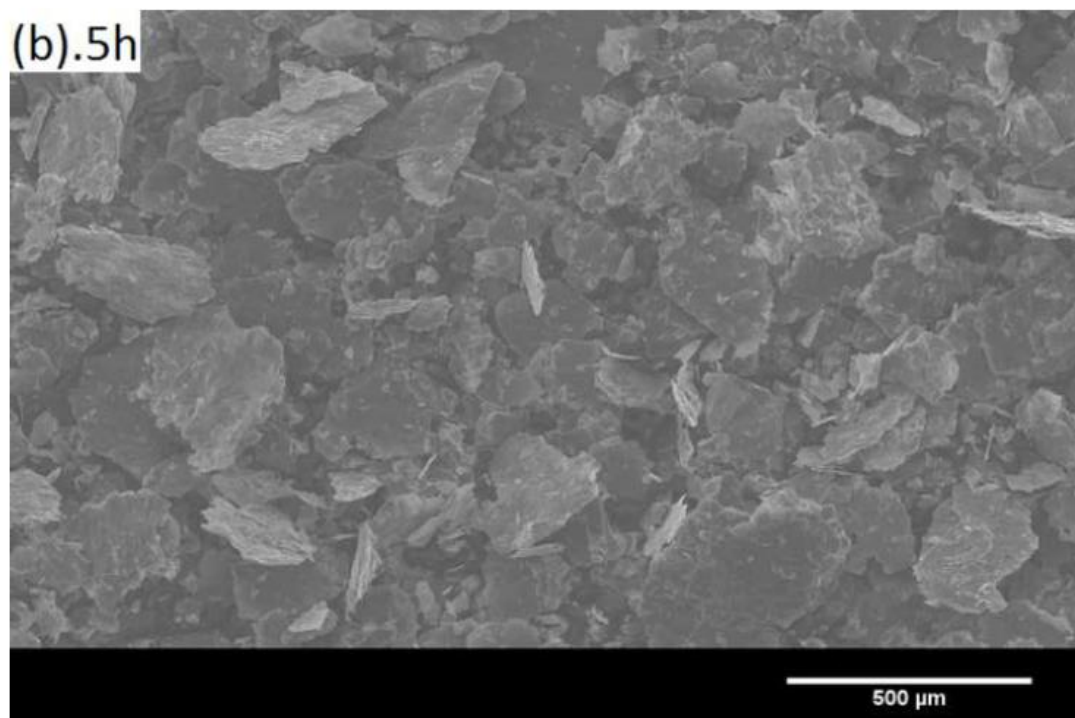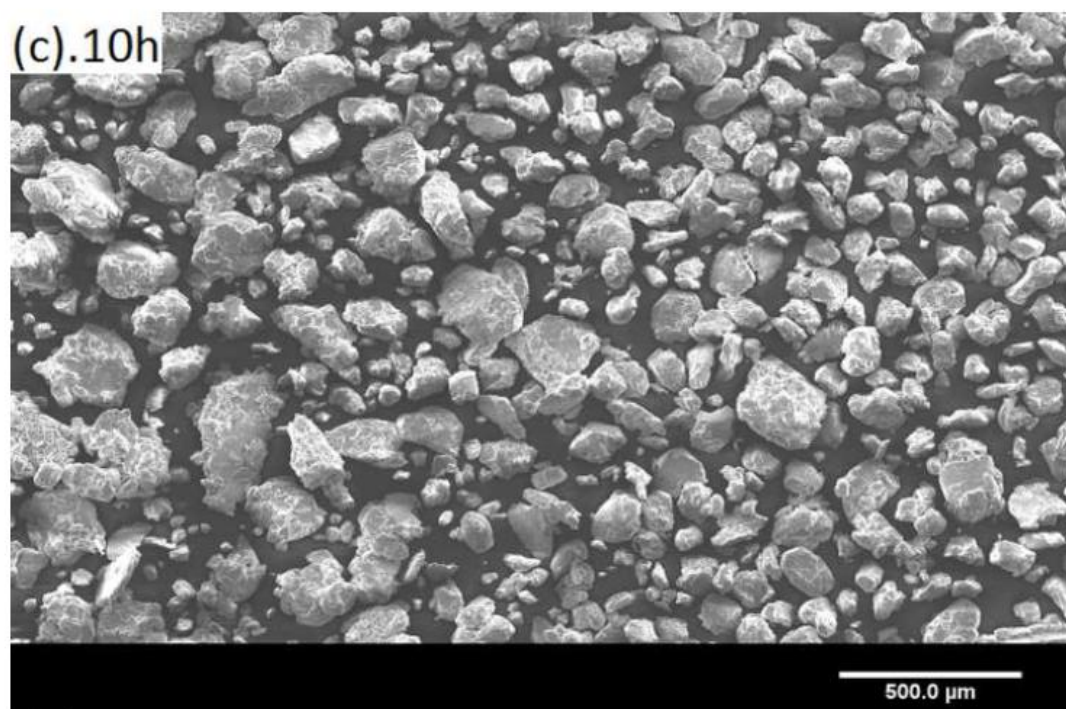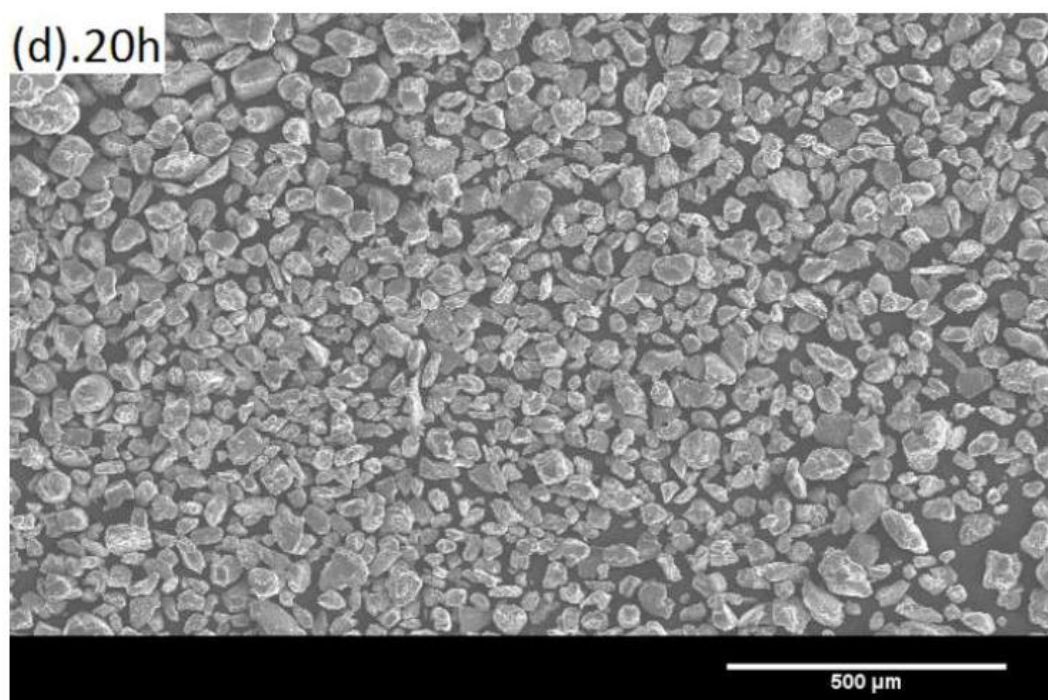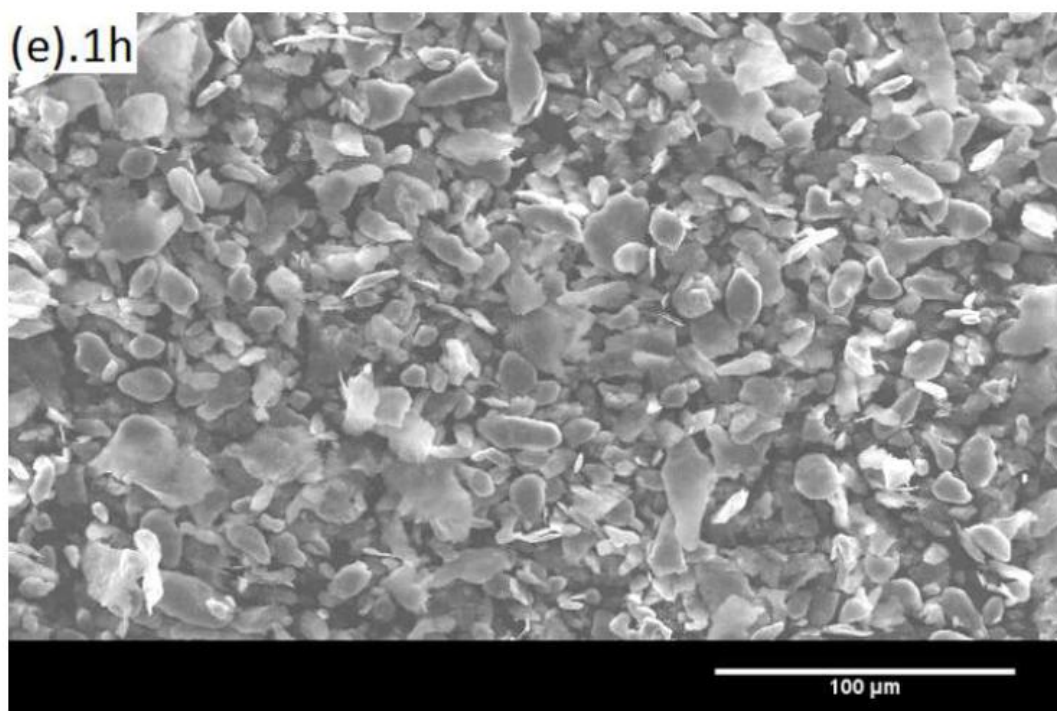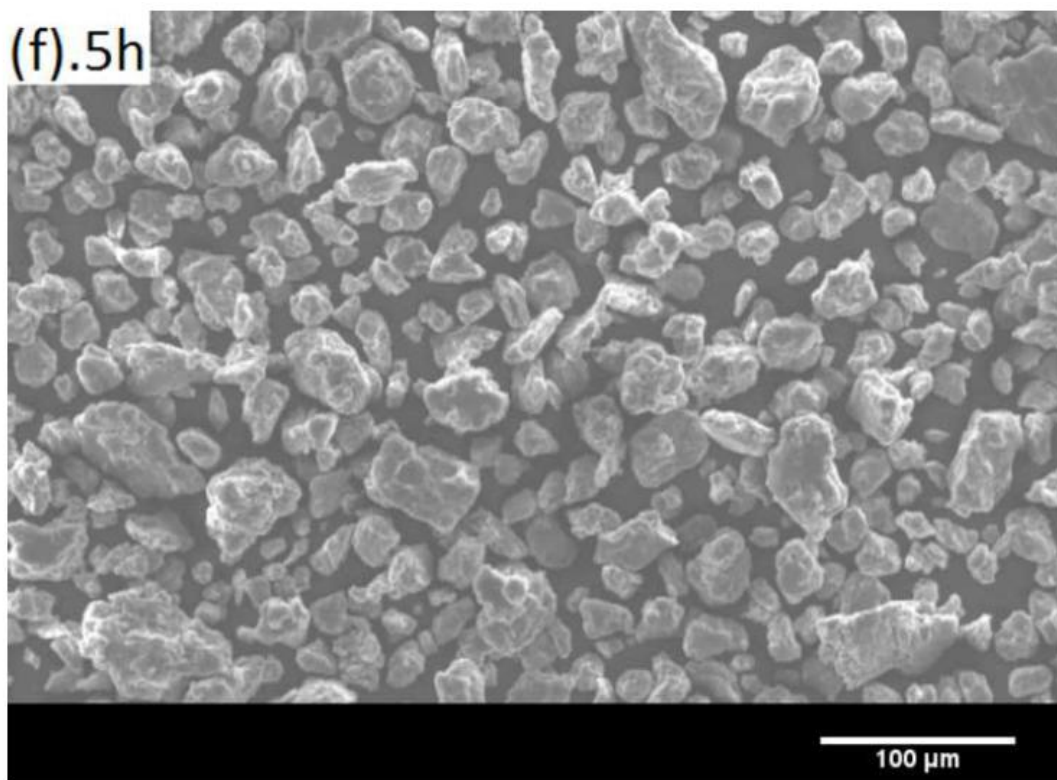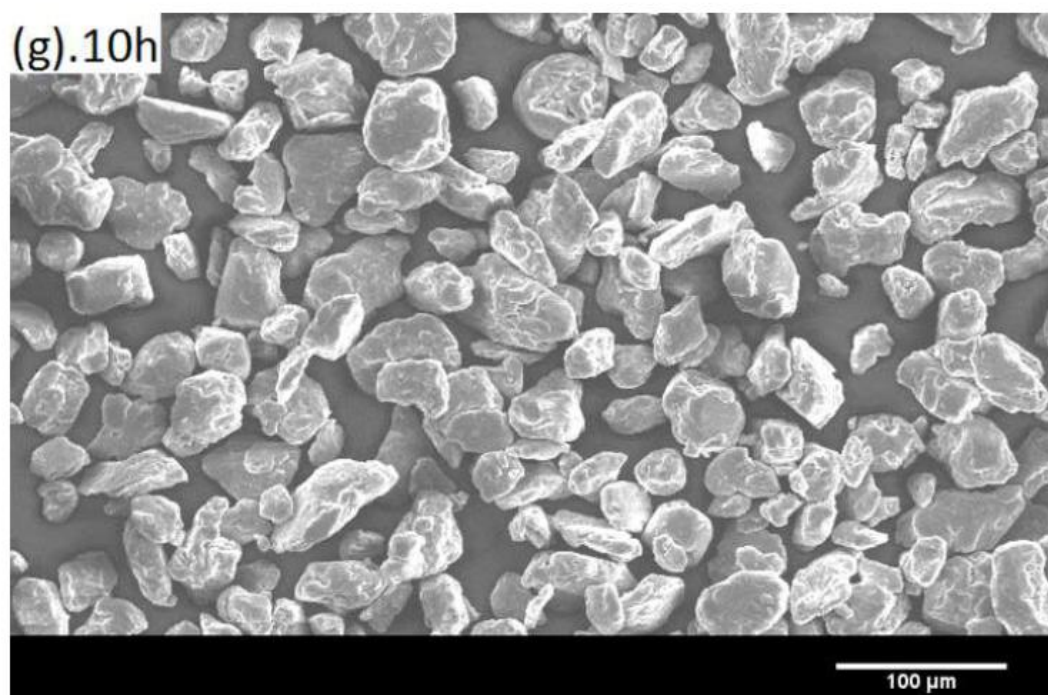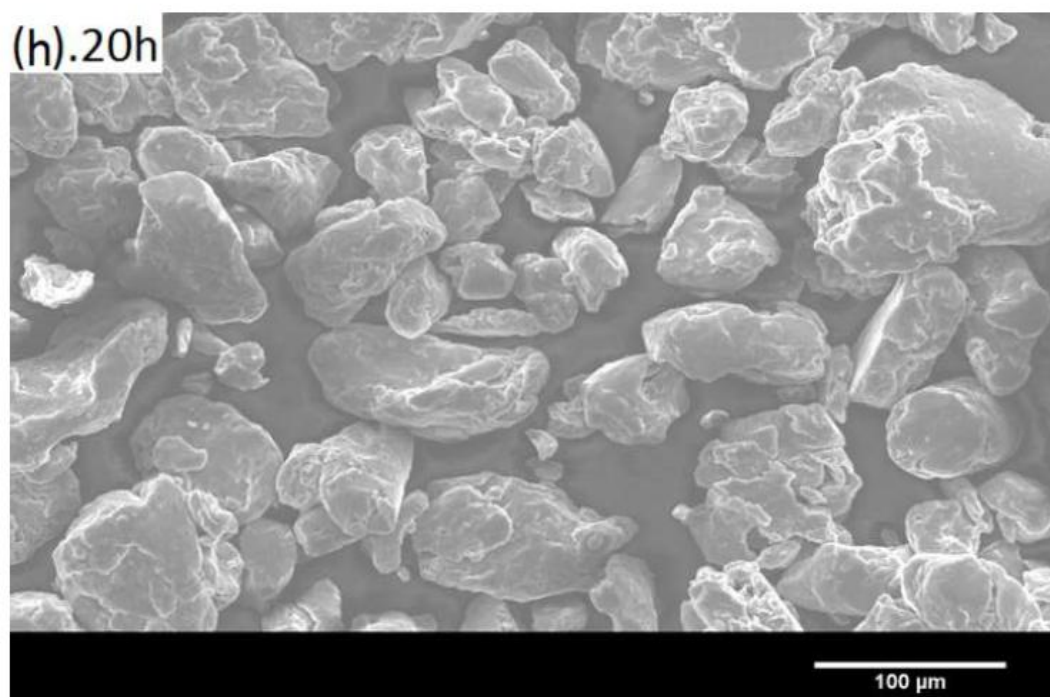
(a).Group A

1 µm

(b).Group B

1 μm

Fig. 2

(b)

30 µm

(c)

40 µm

(d)

10 μm

Fig 3

(b)

1 mm

Fig. 4

Fig. 5

Fig. 6

(b).5h

500 µm

(c).10h

500.0 µm

(d).20h
500 µm

(e).1h

100 µm

(f).5h

100 µm

(g).10h

100 µm

(h).20h

100 µm

Fig. 7

(a).1h

500.0 µm

(b).5h

100 μm

(c).10h

100 μm

(d).1h

100 µm

(e).5h

100 µm

(f).10h

100 µm

Fig. 8

(b).5h-Group A

1 µm

(c).1h-Group B

5 µm

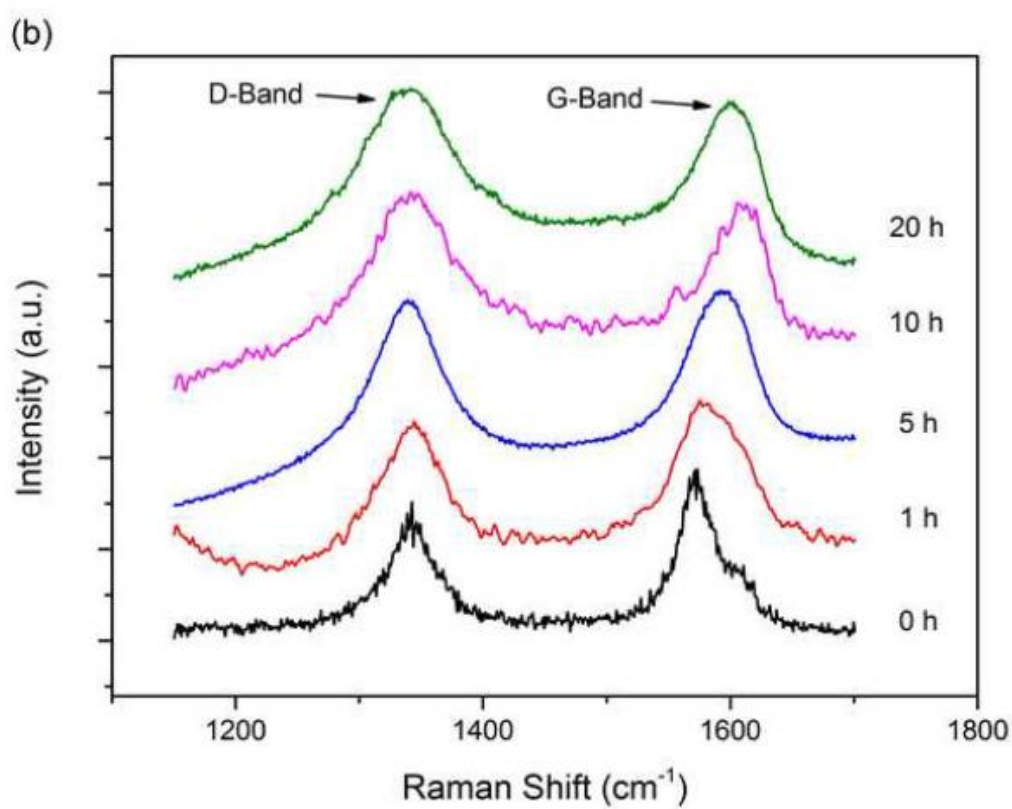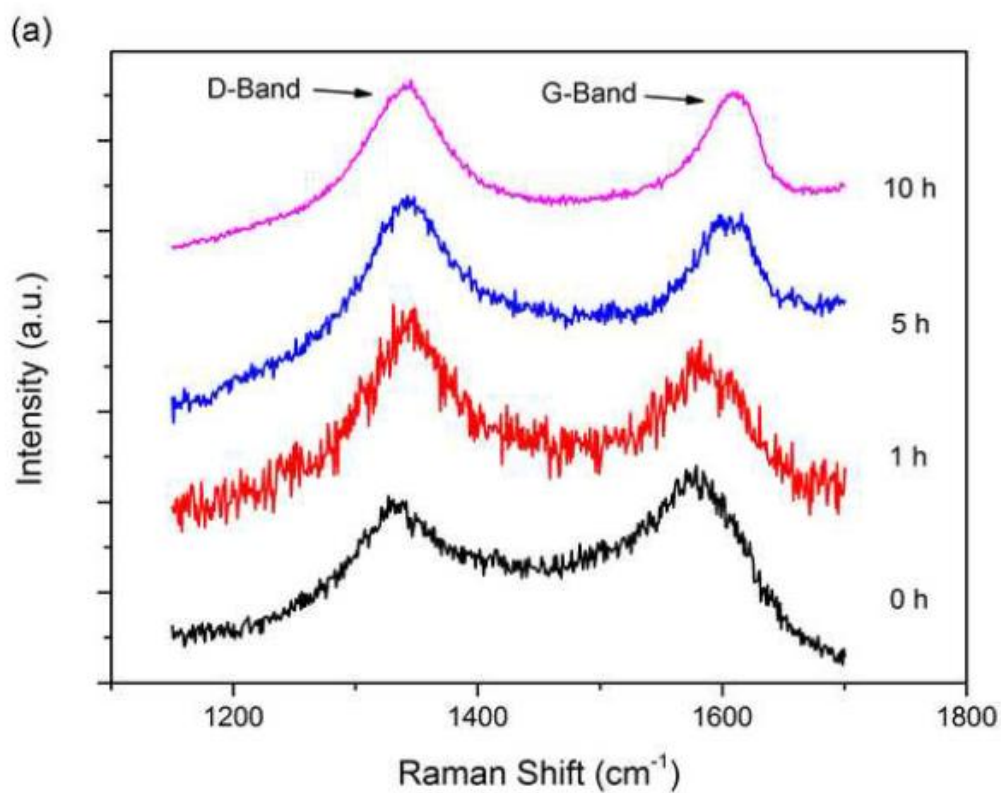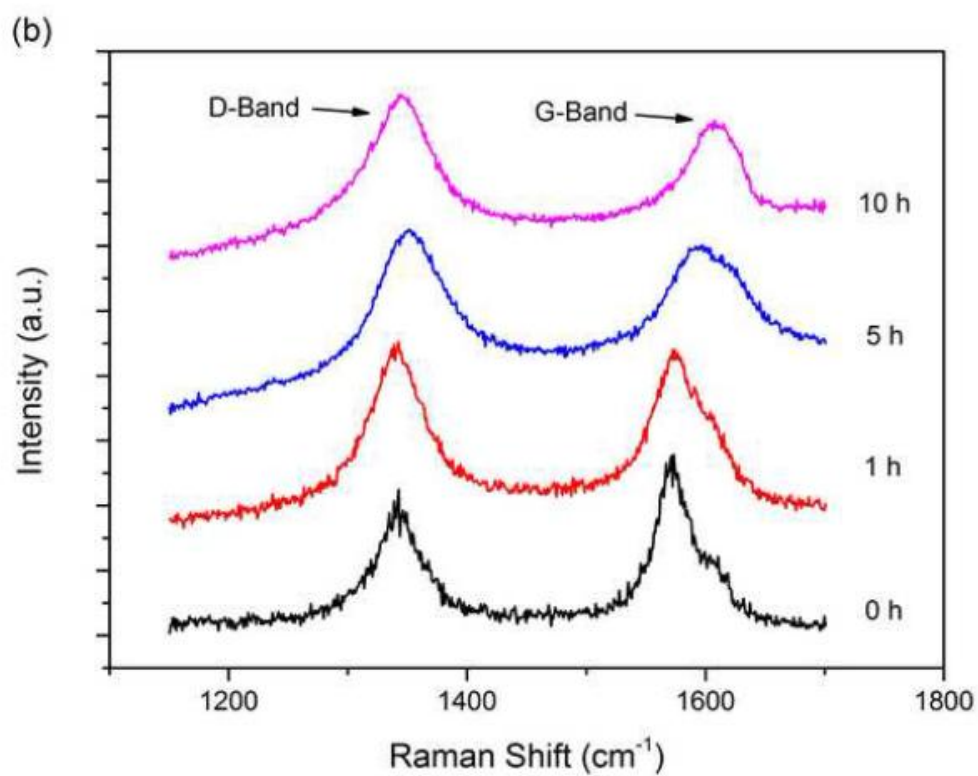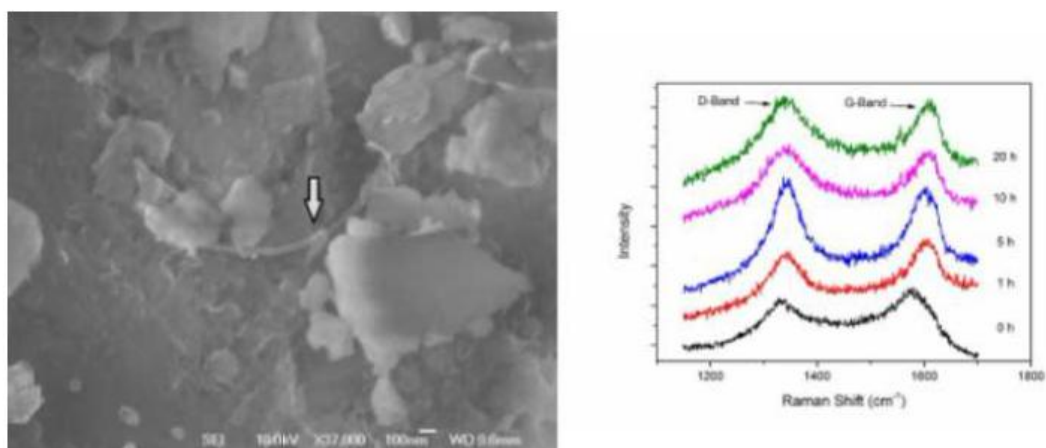(d).10h-Group A

1 µm

Fig. 9

(a)

(b)

Fig. 10

49
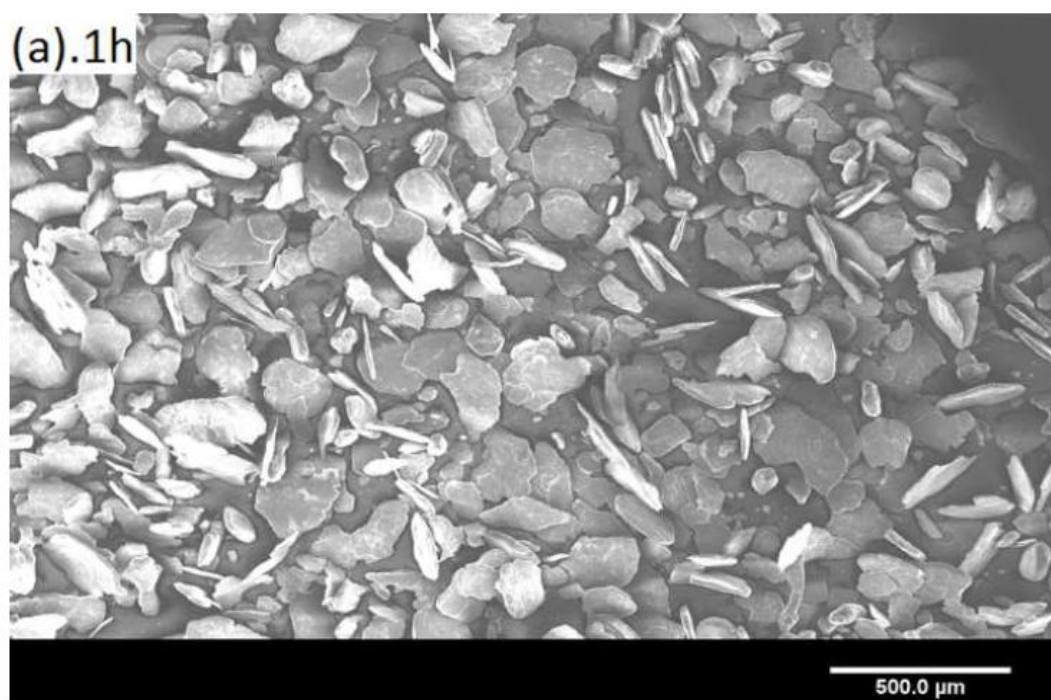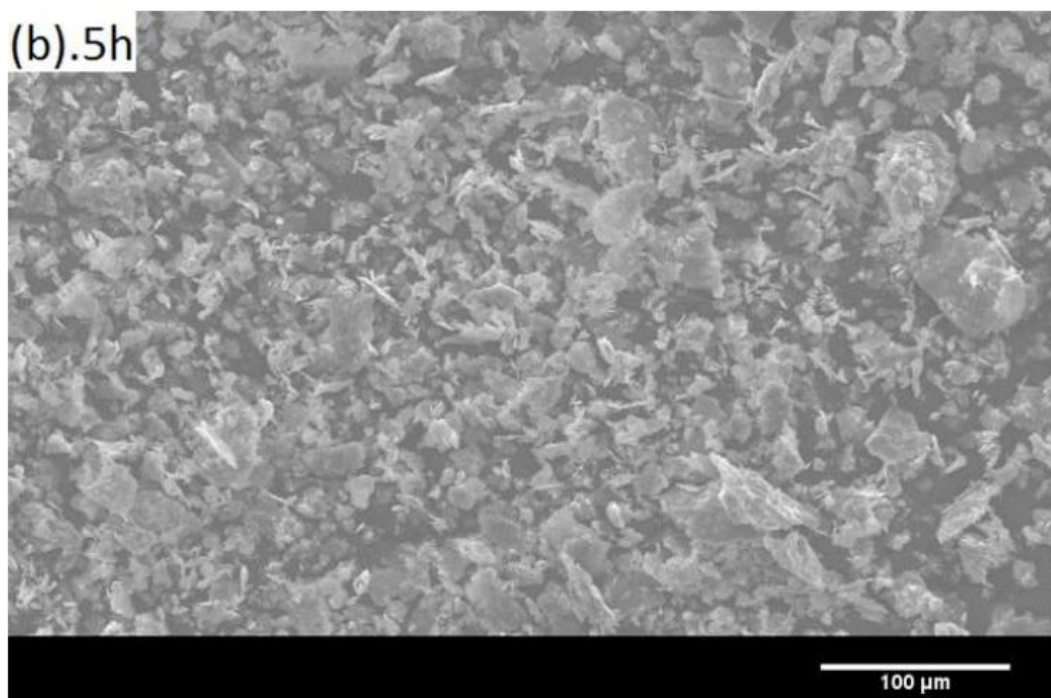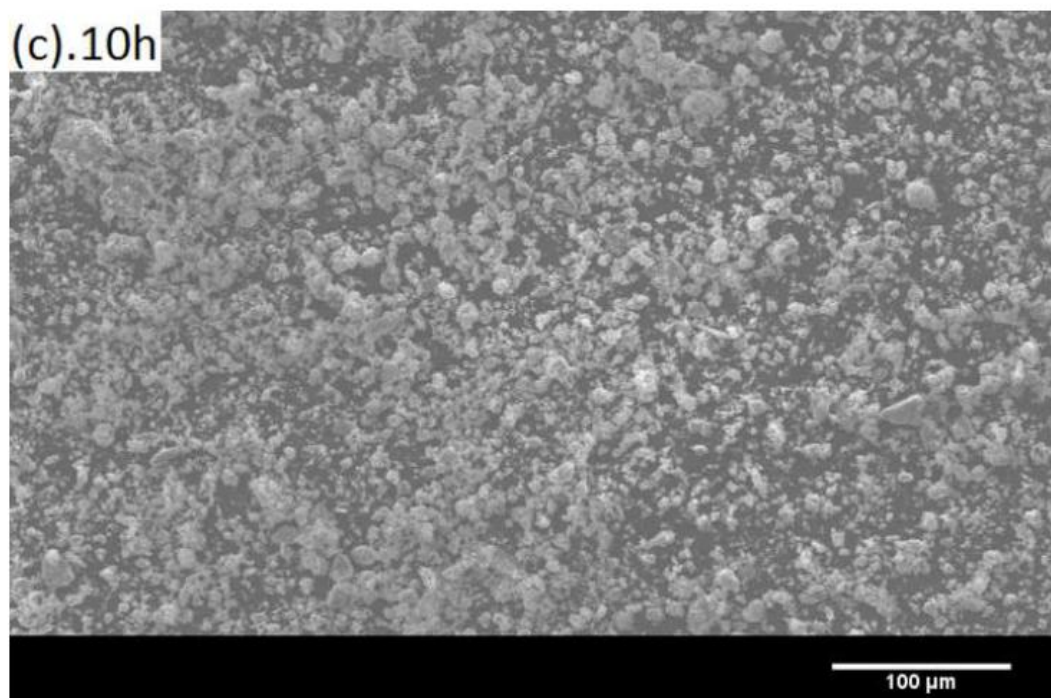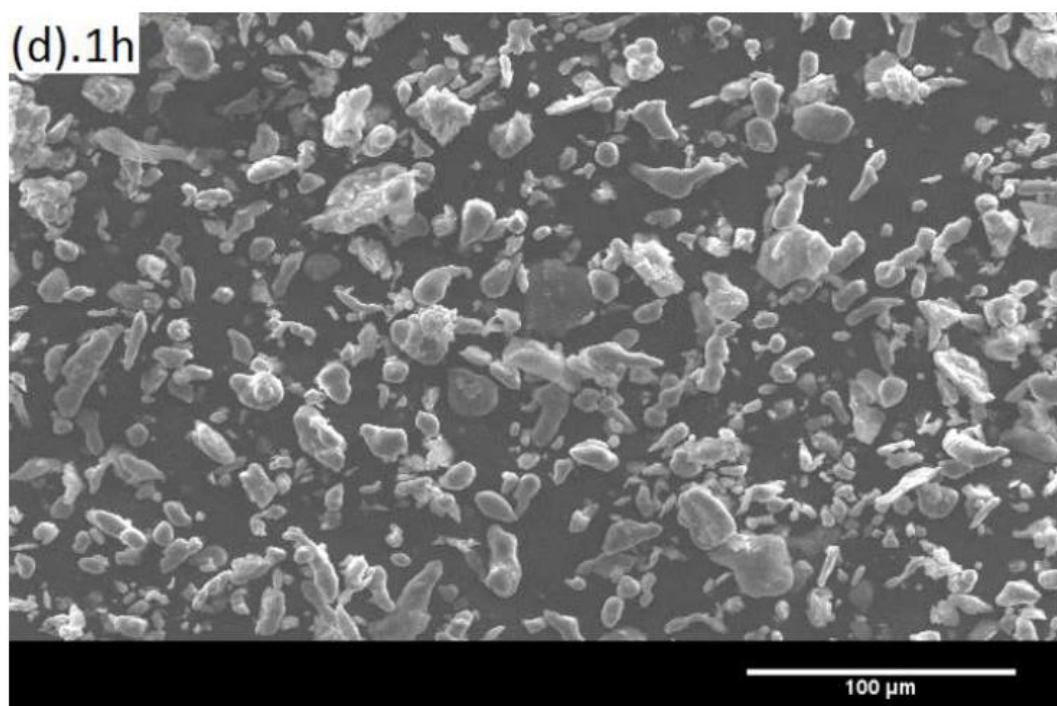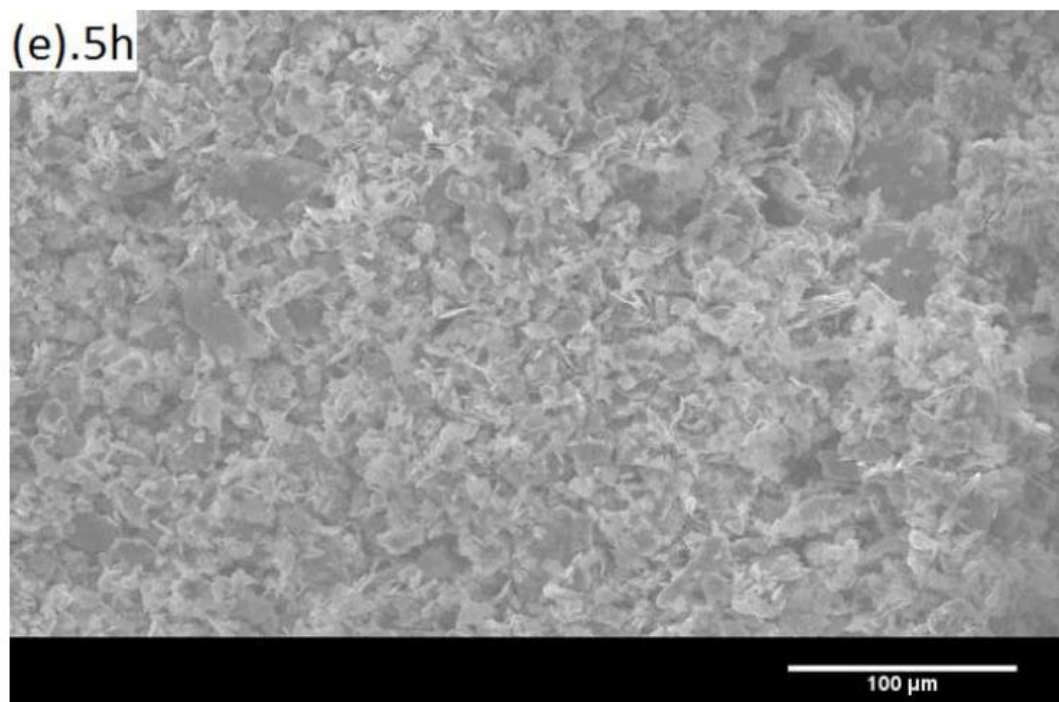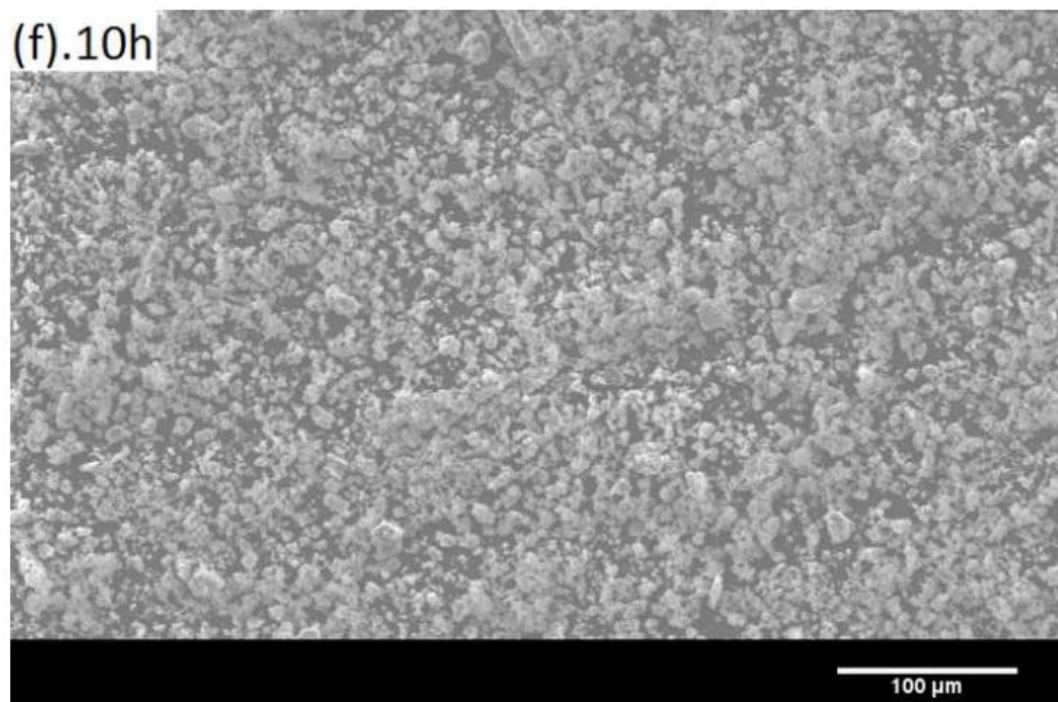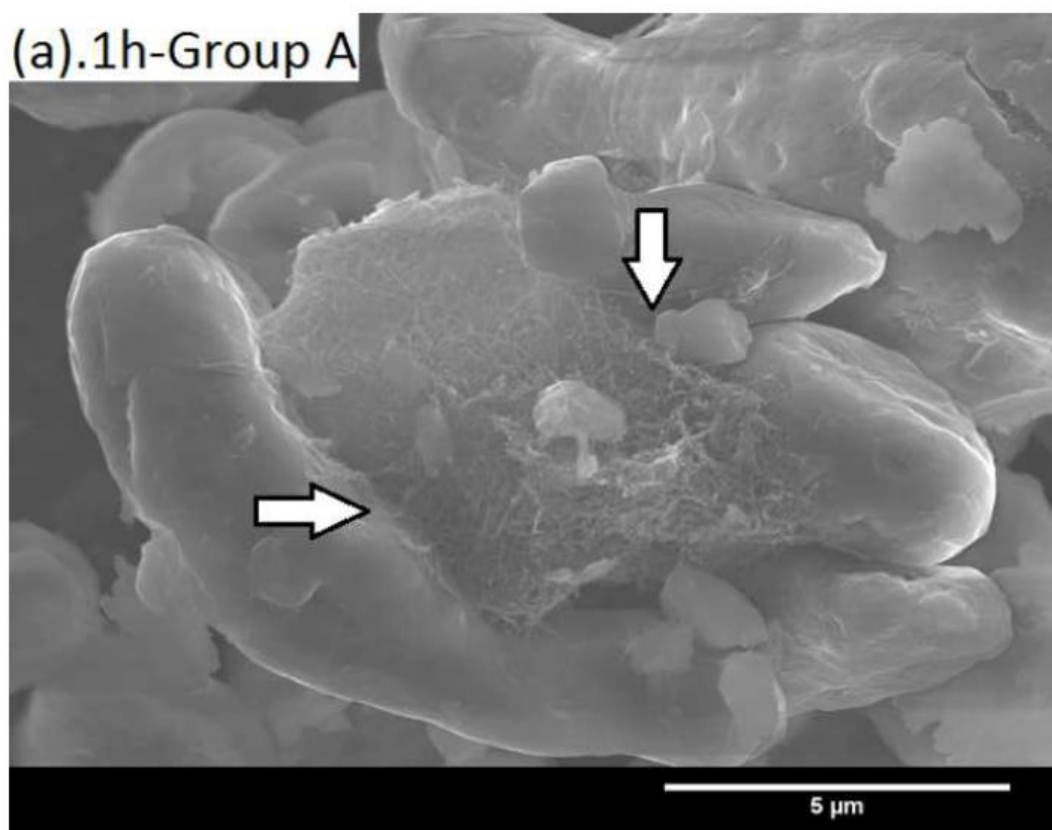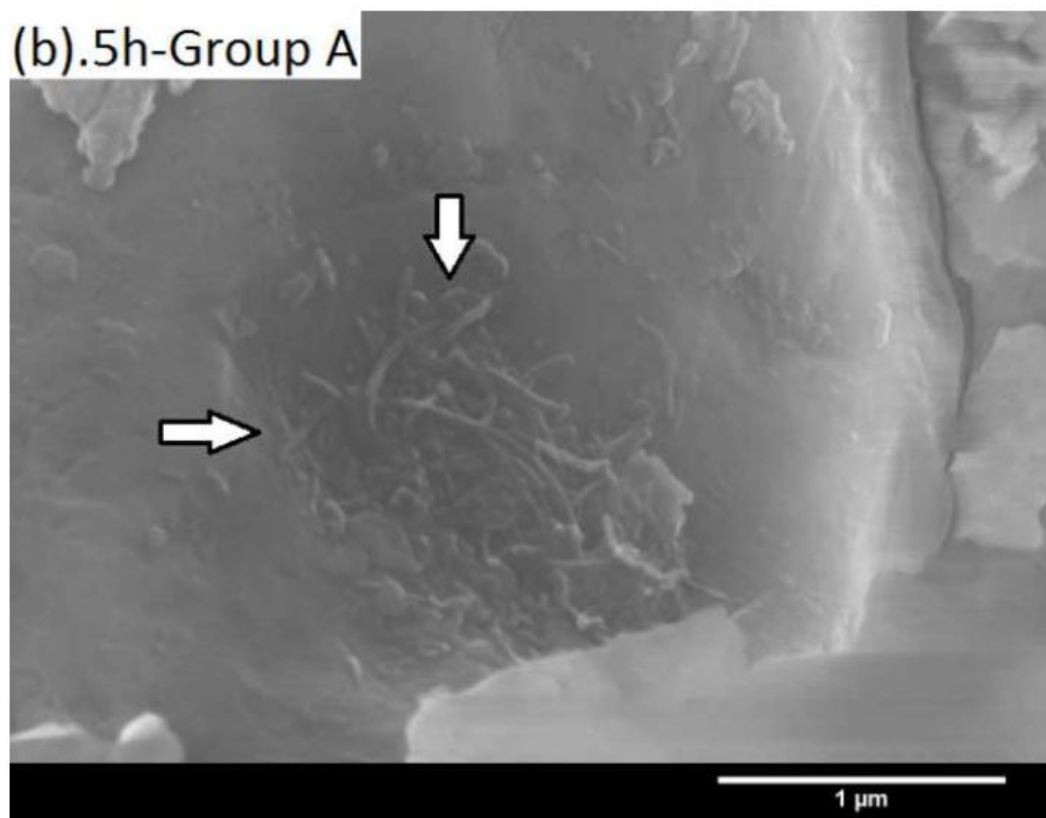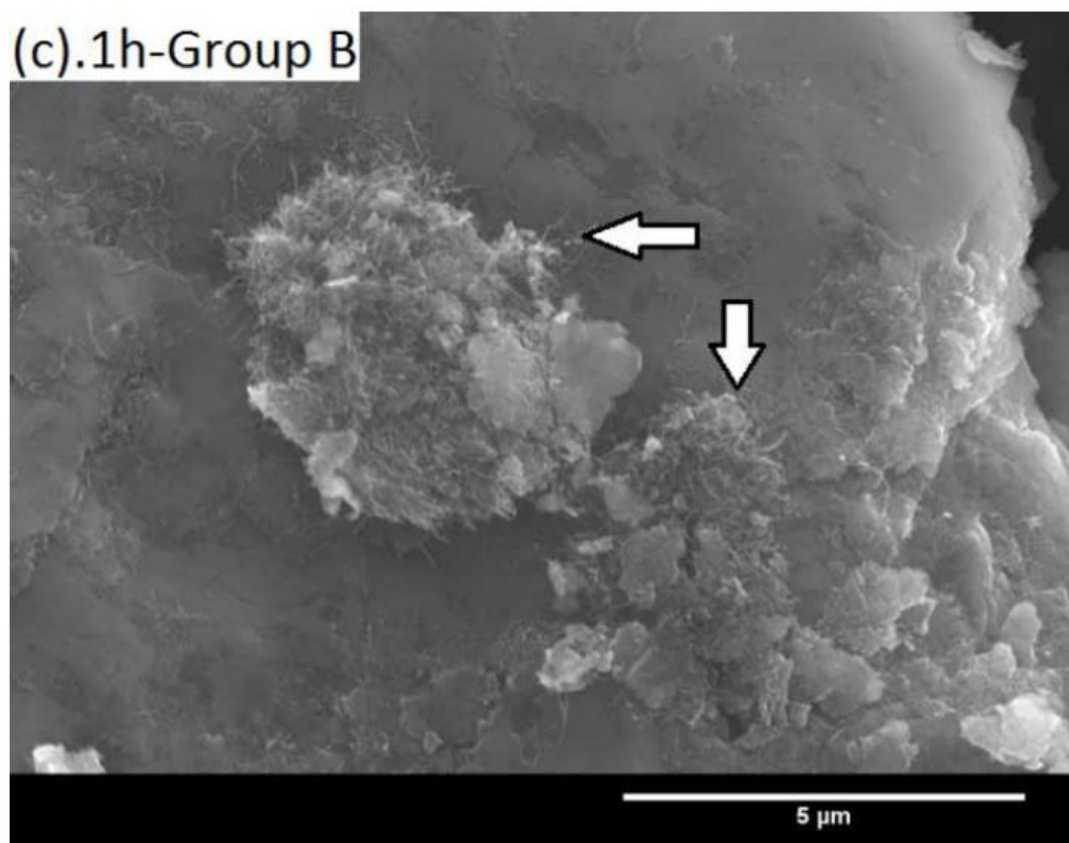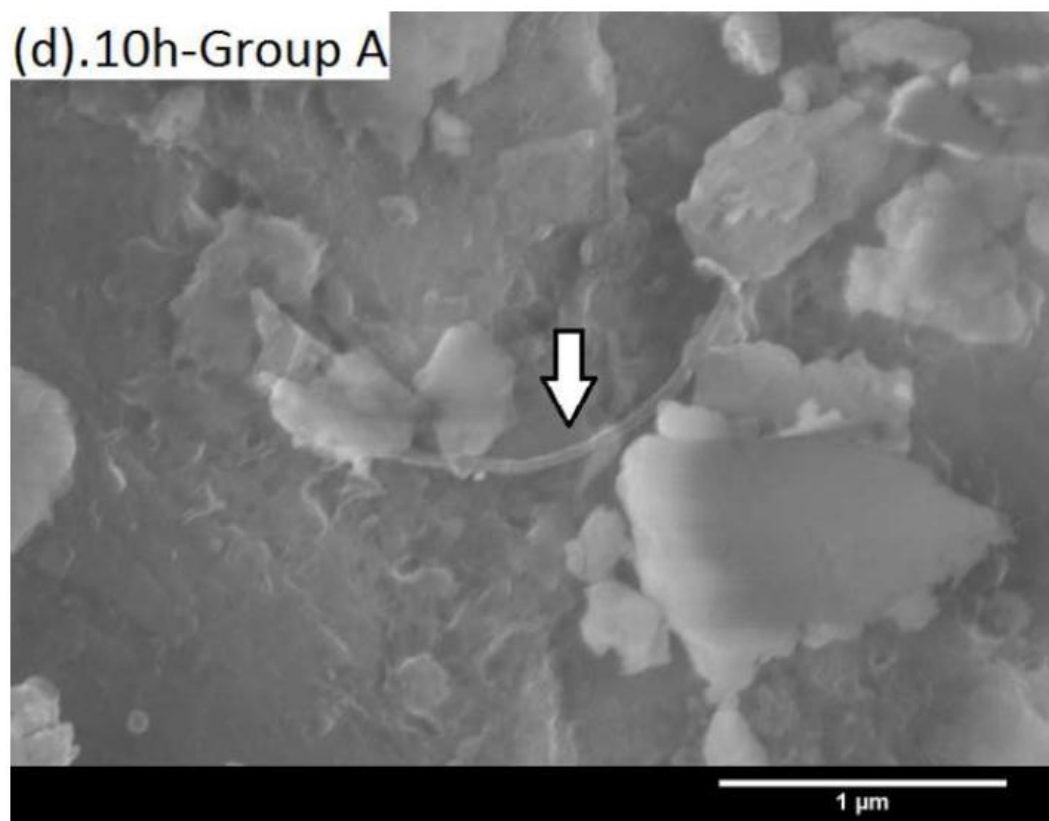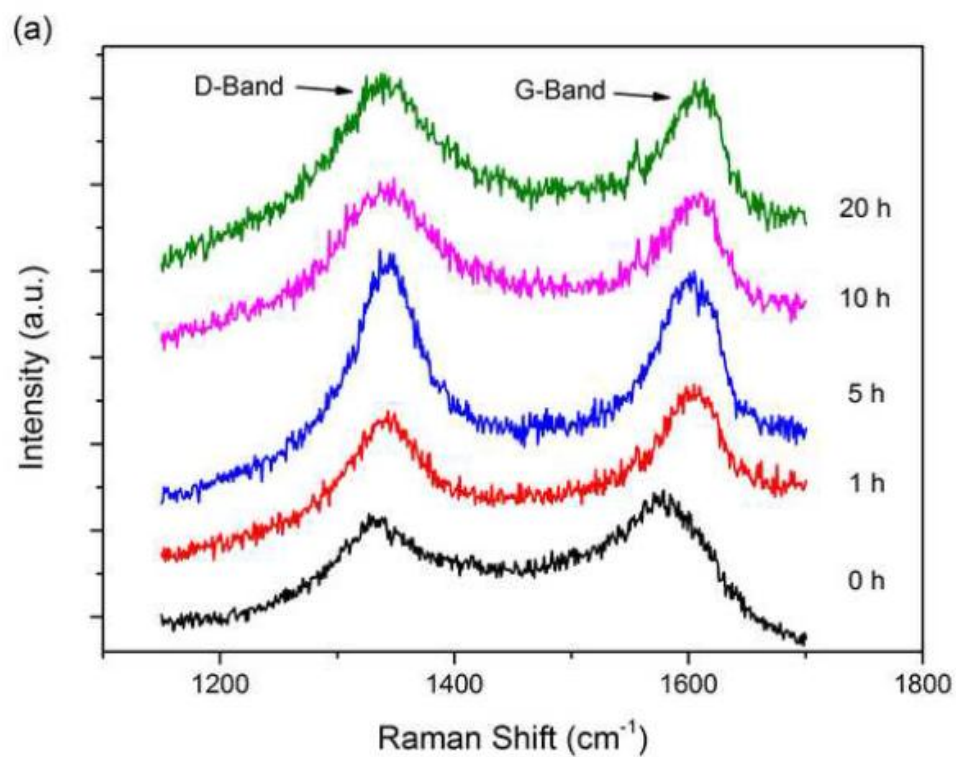
Graphical abstract

ABSTRACT: Carbon nanotubes (CNT) have emerged as a very promising reinforcement for ceramics, polymers and metals. Although the CNT reinforced composites show significant improvement in mechanical, thermal and electrical properties, there are several critical challenges to the effective use of carbon nanotube reinforce composites such as agglomeration of CNT, poor distribution and weak bond between CNT and base matrix. In this paper, mechanical alloying (MA) was applied by the authors to disperse CNT in aluminum matrix. Both stearic acid and ethanol were used as process control agent (PCA) to control the properties of particles. Scanning electron microscope (SEM), Raman spectroscope and particle size analyzer were employed to characterize the size, shape and morphology of CNT-Al composite. The evolutions of CNT and CNT-Al mixture as well as the effect of PCA were studied. The present research indicates that mechanical alloying is an effective way to achieve homogenous distribution of CNT in the Al matrix. Ethanol as process control agent promotes the refinement of Al particles but also increase the damage of CNT during the ball milling process.

Highlights

- Carbon nanotubes were dispersed in aluminum metal matrix by ball milling.

- Process control agent ethanol and stearic acid were added in to the mixture.

- Ethanol induced more defects and damages to the structure of carbon nanotube than stearic acid.

- The microstructure and morphology of aluminum and the evolution of carbon nanotube were studied.